SU-SEL-70-034

AD709069

Spatial Properties of Ionospheric Radio Propagation as Determined With Half-Degree Azimuthal Resolution

by

L. E. Sweeney, Jr.

June 1970

This document has been approved for public release and sale; its distribution is unlimited.

TECHNICAL REPORT NO. 155

Prepared under
Office of Naval Research Contract
Nonr-225(64), NR 088-019, and
Advanced Research Projects Agency
ARPA Order No. 196

Reproduced by the
CLEARINGHOUSE
for Federal Scientific & Technical
Information Springfield Va. 22151

D D C
RECEIVED
JUL 23 1970
C

RADIOSCIENCE LABORATORY

STANFORD ELECTRONICS LABORATORIES

STANFORD UNIVERSITY · STANFORD, CALIFORNIA

SEL-70-034

SPATIAL PROPERTIES OF IONOSPHERIC RADIO PROPAGATION AS DETERMINED WITH HALF-DEGREE AZIMUTHAL RESOLUTION

by

L. E. Sweeney, Jr.

June 1970

This document is approved for public release and sale; its distribution is unlimited.

Technical Report No. 155

Prepared under
Office of Naval Research Contract
Nonr-225(64), NR 088-019, and
Advanced Research Projects Agency
ARPA Order No. 196

Radioscience Laboratory
Stanford Electronics Laboratories
Stanford University Stanford, California

ABSTRACT

In order to determine the influence of oblique ionospheric radio propagation upon the performance (azimuthal pattern) realized by a very large HF array, a 256-element, 2.5 km broadside array has been constructed, and used to receive signals propagated over a 2600 km east-west path from a test transmitter. During implementation of this array, a new technique for matching the lengths of very long feedlines was devised and shown to provide outstanding precision and convenience. It was found that the sensitivity conferred by sweep-frequency CW (SFCW) sounding and the directivity of the receiving array permitted useful ionospheric research to be conducted with transmitted powers as low as 5 mW.

Through the use of SFCW sounding, propagation modes were separated and their azimuthal properties were individually studied as a function of radio frequency with the large array. Daytime studies revealed that single-hop propagation usually appears discrete in azimuth and time delay within the resolution of the system. Ground-reflected modes, on the other hand, are generally spread both in azimuth and time delay, presumably as a consequence of the ground reflections occurring within the Rocky Mountain region.

During quiet conditions, the one-hop F2 low ray was observed to have an angle of arrival usually within 0.25 deg and always within 0.5 deg of the true transmitter bearing. The one-hop F2 high ray was found to commonly arrive south of the low ray. This tendency was hypothesized to be a consequence of ionospheric tilts having north-south slopes which increase with altitude. The plausibility of this explanation was confirmed by three-dimensional computer raytracing with a model ionosphere based upon vertical ionosonde data.

A new propagation mode was discovered which is thought to result from two-hop propagation in which energy travels one hop via high ray and the other via low ray. The existence of such a "combination mode" requires rough scattering at the midpath reflection region (the Rocky Mountains in this case), to enable transfer of energy between high and

low rays. The proposed explanation for the combination mode was substantiated analytically by computer raytracing, and experimentally by operating an HF repeater at the path midpoint.

A new experimental technique was developed which, using SFCW sounding, measures amplitude versus time delay at eight azimuths simultaneously, with each azimuth having the resolution of the full 2.5 km array. The new technique makes extensive use of digital processing, and allows greatly improved flexibility, accuracy and dynamic range compared to previous techniques. In addition, the technique allows the distributions across the array of received signal amplitude and phase to be measured individually for all propagation modes.

Finally, measurement of ionospherically induced doppler shifts versus azimuth for obliquely propagating CW signals demonstrated that, when modes could be resolved in frequency on the basis of their different doppler shifts, they could often be identified on the basis of their azimuthal properties. This was accomplished when receiving with only eight whips spaced uniformly across the 2.5 km aperture. Data were presented in which the one-hop F2 high ray and low ray exhibited discrete doppler spectra, while two-hop F2 produced a spread doppler spectrum.

It was concluded that, during normal daytime conditions, the performance (azimuthal pattern) of a 2.5 km HF array was not significantly affected by ionospheric reflection of single-hop signals received over a 2500 km path. The performance of the array was substantially degraded, however, when it was receiving multihop modes. This degradation was presumably caused by ground reflections rather than by ionospheric reflections.

CONTENTS

Page

I. INTRODUCTION 1

A. Purpose 1

B. Background 1

1. Motivation 1
2. Previous Work 3

C. Approach Used in the Present Study 8

II. EXPERIMENTAL FACILITIES AND TECHNIQUES 11

A. Receiving Site 11

B. Transmitting Site 14

C. Sweep-Frequency CW (SFCW) Sounding 14

III. LOW-POWER OBLIQUE SOUNDINGS 19

A. Experimental Design 19

B. Experimental Results 19

IV. AZIMUTHAL DISTRIBUTIONS OF IONOSPHERIC MODES 27

A. Experimental Procedure 27

B. Experimental Results 29

C. Southerly High Ray Deviations 39

D. Summary and Discussion 41

V. A NEW PROPAGATION MODE 43

A. First Observations of a New Mode 43

B. Explanation of the New Mode 43

C. Additional Observations of the Combination Mode 47

D. Verification of the "Combination-Mode" Explanation . . . 49

VI. DIGITAL FORMATION OF MULTIPLE BEAMS 53

A. Experimental Arrangement 55

B. Data Processing 57

C. Examples of Experimental Results 59

CONTENTS (Cont)

Page

VII. DIGITAL MEASUREMENT OF IONOSPHERIC DOPPLER VERSUS AZIMUTH . . 65

A. Experimental Arrangement 65

B. Data Processing. 65

C. Experimental Results 67

VIII. CONCLUSION. 75

A. Summary of Results 75

B. Discussion and Evaluation. 77

C. Conclusions. 77

D. Recommendations for Future Work. 77

Appendix. A NEW TECHNIQUE FOR FEEDLINE MATCHING 79

REFERENCES 89

TABLE

Number Page

1 Theoretical 3 dB, 6 dB, 10 dB and 20 dB beamwidths versus frequency of the Los Banos receiving array 12

ILLUSTRATIONS

Figure		Page
1	Photograph of the 256-element, 2.5 km receiving array located near Los Banos, California. The main data-processing van is visible in the distance at the left. . .	10
2	Block diagram of the beam-forming system for the receiving array.	13
3	Block diagram of a sweep-frequency CW (SFCW) sounder . . .	17
4	Low-power Bearden-to-Los Banos oblique soundings made on 26 Sept 1968 at about 1500 UT (0800 midpath time) using the full 256-element receiving array	20
5	Low-power oblique soundings made on 3 Oct 1968 at about 1640 UT (0940 midpath time) showing the dependence of record quality upon the directive gain of the antenna. . .	22
6	Low-power (5 mW) soundings made on 3 Oct 1968 at about 1700 UT (1000 midpath time) showing the dependence of record character upon the main lobe direction of the 256-element array.	23
7	Low-power soundings made on 3 Oct 1968 at about 1700 UT (1000 midpath time) illustrating the change in record character produced by broadening the antenna beamwidth . .	24
8	Block diagram of the system used to produce displays of time delay vs azimuth (azimuth scans).	28
9	Displays of time delay vs azimuth (azimuth scans) at odd frequencies from 9 MHz to 31 MHz taken on 28 Mar 1969 at about 2230 UT (1530 midpath time). Beamwidths (10 dB) of the receiving array are listed to aid in interpretation. See Figure 10 for an ionogram taken at about this time . .	30
10	Ionogram taken 28 Mar 1969 at 2246 UT (1546 midpath time) to aid in interpretation of Figure 9	31
11	Ionogram taken 25 Aug 1969 at 2150 UT (1450 midpath time) just prior to the measurements plotted in Figure 12. . . .	34
12	Plot of the angle of arrival vs time for the one-hop F2 low ray (1F2L) and the one-hop F2 high ray (1F2H) taken at 23 MHz on 25 Aug 1969. See Figure 11 for an ionogram taken at about this time	35

ILLUSTRATIONS (Cont)

Figure		Page
13	Arkansas-to-Los Banos ionogram (left) and azimuth scan at 14.5 MHz (right) taken 30 Sept 1969 at about 2000 UT (1300 midpath time).	36
14	Angles of arrival vs time for the various ionospheric modes propagating at 14.5 MHz on 30 Sept 1969.	37
15	Plot of height vs latitude for contours of constant plasma frequency (constant electron density) derived from a monthly mean of local noontime measurements taken during April of 1959. (Taken from Ref. 21)	38
16	Computer model for ionosphere of Figure 15	40
17	Plot of angle of arrival vs ground range, with frequency as a parameter, derived by three-dimensional computer raytracing using the model ionosphere of Figure 16	40
18	Ionograms taken 2 May 1968 at about 0315 UT (2015 midpath time) with the receiving array directed to an azimuth of 90 deg	42
19	Simplified geometry for two-hop oblique ionospheric propagation at a single frequency.	44
20	Two-hop ionogram generated by computer raytracing for a 2600 km path with equal length hops of 1300 km each. . . .	44
21	Computer-generated two-hop ionogram for a 2600 km path having one hop of 1200 km and the other hop of 1400 km . .	46
22	Superposition of two-hop ionograms from Figures 20 and 21.	46
23	Ionogram taken 2 May 1969 at about 2200 UT (1500 midpath time). The receiving array was directed to an azimuth of 92 deg, 2 deg south of the true transmitter bearing. . . .	48
24	Soundings emphasizing the two-hop F2 propagation mode taken 30 sec apart on 2 May 1969 at about 2120 UT (1420 midpath time). The receiving array was again directed to an azimuth of 92 deg.	48
25	Soundings showing echoes from a repeater operating near the midpath point of the Bearden-to-Los Banos path	50

ILLUSTRATIONS (Cont)

Figure		Page
26	Block diagram of the eight-channel receiving and digital recording system for the Los Banos array	54
27	Basic digital data-processing scheme for determining signal spectrum vs azimuth	56
28	Block diagram of the complete digital processing scheme, showing modifications to the basic scheme of Figure 27 . .	56
29	Digitally processed ionogram for a sounding received with a single Los Banos subarray on 28 Mar 1969 at 2236 UT (1536 midpath time).	60
30	Digitally processed displays of received signal amplitude vs time delay at 9 azimuths for various frequencies selected from the ionogram of Figure 29.	61
31	Digitally processed displays of received signal amplitude vs time delay at 9 azimuths (bottom) and distributions of amplitude and phase across the receiving array (top) for selected modes from the ionogram of Figure 29.	63
32	Ionogram taken 15 Jan 1970 at about 2130 UT (1430 midpath time).	66
33	Digitally processed displays of received signal amplitude vs frequency at 9 azimuths (top) and distributions of amplitude and phase across the array for the strongest frequency component (bottom) with a calibration signal applied to the input of the receiving system	68
34	Digitally processed displays for a CW signal received at a frequency for which only one-hop F2 low ray (1F2L) was propagating.	70
35	Digitally processed displays for a CW signal received at a frequency for which both one-hop F2 low ray (1F2L) and two-hop F2 (2F2) were propagating.	71
36	Digitally processed displays for a CW signal received at a frequency for which both one-hop F2 low ray and high ray (1F2L and 1F2H, respectively) were propagating	72
37	Block diagram of the feedline matching system.	80
38	Demonstration of the sensitivity of the feedline matching technique when comparing two 4800 ft feedlines	86

ACKNOWLEDGMENT

I wish to express special thanks to Professor O. G. Villard, Jr. for his guidance and encouragement throughout this work. I am grateful to Professor L. A. Manning and Professor R. J. Smith for their assistance and suggestions in improving the technical quality of the manuscript. My thanks also go to Mrs. Mabel Rockwell and to Miss Jane King for their help in preparing the finished report.

This research was supported by the Advanced Research Projects Agency through the Office of Naval Research, Contract Nonr-225(64).

I. INTRODUCTION

A. PURPOSE

The purpose of the research described in this report was to investigate experimentally the properties of oblique ionospheric radio propagation which could degrade or limit the performance realized by a very wide-aperture (2.5 km), high-frequency broadside array. "High-frequency" (HF) refers to the frequency band from 3 MHz to 30 MHz. A broadside antenna array is one whose main lobe direction is roughly perpendicular to the line of its elements. Since the performance of such an array can most meaningfully be measured in terms of its horizontal pattern (beamwidth and sidelobe levels), the emphasis of this study was upon the apparent azimuthal pattern of an array when receiving ionospherically propagated radio energy emanating from a point source.

B. BACKGROUND

1. Motivation

The specific motivation for this work was to establish the feasibility of using HF broadside arrays an order of magnitude longer than any employed previously for ionospheric radio propagation. The primary effects (in free space) of increasing the length of an array while maintaining a constant physical interelement spacing are first, that directive gain varies directly with length, and second, that the beamwidth varies inversely with length [Ref. 1, p. 877].

There are several reasons why the performance obtainable with larger arrays is desirable. Probably the most important of these reasons, in recent years, is a consequence of an ever-increasing number of stations which use the HF spectrum. The limited number of frequency allocations available has led to more and more sharing of channels, and to greatly increased interference between stations. Since interference is simply a form of unwanted noise, this situation has, for some

services, seriously degraded the signal-to-noise ratios obtainable over ionospheric channels. Furthermore, the conduct of ionospheric research has been complicated in recent years by the fact that increased interference has reduced the flexibility and sensitivity of broadband ionospheric sounders. Obviously, increasing transmitter power in an effort to retrieve the signal-to-noise ratios lost to interference in some systems will only aggravate the interference to other systems.

A better approach is to increase the directive gains of the antennas used by HF stations. Doing so can strengthen the received signal from a desired station while reducing the interference both to and from other stations. For transmitting arrays, the increased gain means a higher effective radiated power (ERP) in the desired direction, thus providing increased signal strength at the receiver. In addition, less power is radiated in other directions, which reduces interference to other stations. In receiving arrays, increased directive gain improves sensitivity to signals from a desired direction while reducing sensitivity to unwanted signals and noise coming from other directions.

Although it is desirable to increase the directive gains of arrays used in ionospheric radio, it is not clear that the ionosphere in practice will support a substantial increase in such gains. A broadside array is designed to transmit and receive plane waves. This means that, for any frequency, any phase difference between the currents in two array elements is proportional to the spacing between the elements. (This condition is referred to as "linear phase.") If the phase fronts of transmitted plane waves are seriously distorted by ionospheric propagation so that the phase distribution across the array is not linear, the performance of the array in receiving that particular signal will be degraded.

From another viewpoint, if the discrete directions of signal and noise sources are modified by propagation so that they arrive from a spread of directions greater than the array beamwidth, then the potential for enhancing the desired signal and rejecting the unwanted signals and noise by increasing the directive gain of the array will be reduced. Furthermore, if a desired signal arrives from a discrete direction which

wanders about with time, the theoretical directive gain of the array will not be realized unless the array beamwidth is sufficiently wide always to include the direction of arrival of the signal, or unless the main lobe of the array can be slewed to cope with drifts in signal direction.

This research was undertaken to determine experimentally to what extent ionospheric propagation can influence the performance of very large HF arrays.

2. Previous Work

Prior to the author's work described herein, few results have been published which are directly applicable to predicting the performance of a 2.5 km broadside array. No such array had previously been used in an oblique ionospheric application. In addition, no measurements of ionospherically propagated signals had been conducted which bore directly upon this problem. However, a number of earlier results may be extrapolated so as to bear indirectly upon the feasibility of very large arrays. In addition, past experience of other workers assists greatly in defining those aspects of propagation which are most important to this problem.

One factor of extreme importance is the separation and identification of the individual ionospheric multipath components or modes. This point was emphasized with respect to the improved performance of direction finders when modes were resolved by Hayden [Ref. 2] and Gething [Ref. 3]. Bowhill [Ref. 4] observed that the correlation between received signal amplitudes at antennas spaced 600 ft apart was much higher for a pulsed signal than for a CW signal. He concluded that most of the space diversity effect in long-distance CW transmissions arises through interference between the various modes. Ames [Ref. 5] sampled the amplitude of received signals at points along an L-shaped aperture having one leg 1000 ft long and the other 1200 ft long. He was able to deduce the tilts of ionospheric layers by examining the patterns of interference between reflected modes as observed along the ground. The fact that this was possible one-third of the

time on an 1840 km path indicated that the individual modes had reasonably linear phase across the array at those times. Hayden [Ref. 2] demonstrated theoretically that the superposition of two or more plane waves, having the same frequency but arriving from different directions, can produce nonuniform amplitude and distorted phase distributions across an array. While a broadside array could realize its ideal performance in receiving any of the plane waves individually, this performance could probably not be realized for all waves simultaneously. Consequently, a very large array might clearly perform well for receiving individual modes, while its performance would be doubtful or at least difficult to interpret when receiving interfering modes.

The work of Bramley and Ross [Ref. 6] and Bramley [Refs. 7, 8, 9] is of particular interest in respect to the current subject. In their work, two direction finders spaced 27 km apart were used for angle-of-arrival studies of obliquely propagated signals. Pulse-modulated transmissions were used to separate modes. Each direction finder consisted of four elements uniformly spaced around the circumference of a circle 100 m in diameter. Two types of fluctuation in signal direction of arrival (azimuth) were observed: rapid second-to-second fluctuations, and slow changes having a quasi-period of many minutes (typically 20 min). The rapid fluctuations are attributed to the inability to completely resolve modes, and to small-scale irregularities in the lower part of the E region of the ionosphere. The slow variations are thought to be caused by large-scale tilts in the F layer.

Comparison of observations for a 2100 km path made with the 100 m instrument to those made with a narrow-aperture Adcock direction finder [Ref. 9] showed that the influence of the rapid fluctuations on the deduced bearings was reduced dramatically when the element spacing was increased. (This reduction was further substantiated by Bain [Ref. 10] who made measurements using a four-element direction finder like Bramley's except with a diameter of 180 m.) This result implies that the phase difference between elements produced by the rapid fluctuations is to some extent independent of element spacing. In Bramley's data at 11 MHz, this phase difference was apparently confined

to within ± 24 deg of the mean value. Such a range of phase across a large broadside array will not seriously degrade its performance [Ref. 11]. It is conceivable, then, that the rapid variation could be averaged out spatially by a large array having many elements, thus eliminating the need for time averaging for the same purpose.

For one-hop F2 low ray and high ray the slow bearing drifts observed by Bramley for the 2100 km path were quite small in magnitude and confined to a range of 0.5 deg for periods on the order of an hour. This implies that the average bearing of a signal could be expected to remain for a long time in the main beam of an array having a beamwidth of 0.5 deg.

Using the two direction finders spaced by 27 km, Bramley and Ross discovered that the two stations exhibited extremely close correlation so far as the slowly changing directional deviations were concerned [Ref. 6]. In a later experiment [Ref. 7] Bramley concluded that the measured directions were uncorrelated at points on the ground separated by 92 km. This implies that ionospherically propagated signal wavefronts may be essentially linear for distances in excess of 30 km. Such an implication is extremely encouraging to the prospect of using very large HF arrays.

Another significant result of Bramley's work is that two-hop modes often exhibit substantially less stable bearings than one-hop modes, and that the amount of fluctuation in the bearing is somewhat more severe when the midpath reflection is on land than on sea [Ref. 8]. This implies that the performance of a very large array may be better for one-hop modes than for two-hop modes, and that the two-hop performance may depend upon the actual path.

In practice, the largest broadside arrays used for oblique ionospheric propagation have been less than 1400 ft long. Two examples of such arrays are the University of Illinois Wullenweber direction-finding system [Ref. 2] and the Environmental Science Services Administration (ESSA) high-resolution scan system [Ref. 12].

The Illinois Wullenweber has 120 elements uniformly spaced around the circumference of a circle 955 ft in diameter. At any

instant of time 40 adjacent elements are combined to form a broadside array 814 ft long. The ESSA system includes a 25-element broadside array which is 1392 ft long. No serious degradation of performance is observed for either of these arrays during normal propagation conditions, thus lending credence to the expectation that large multielement arrays can spatially average out the effects of rapid fluctuations in direction of arrival of signals of the type observed by Bramley.

For completeness it should be mentioned that two very large endfire arrays have previously been used successfully for HF ionospheric propagation. An endfire array is one whose main lobe azimuth is directed along the line of its elements. It primarily provides vertical-angle resolution rather than azimuthal resolution. The MUSA (Multiple Unit Steerable Antenna) array [Ref. 13] consisted of 16 rhombics with 200 m spacing between corresponding parts of adjacent elements. Its total length was nearly 3.2 km. The ISCAN (Inertialess Steerable Communication Antenna) array [Ref. 14] contained 24 vertical dipoles arranged in a straight horizontal line, nonuniformly spaced, and spread over a distance of 1920 m. Both of these arrays were intended to permit separation in vertical angle of simultaneously arriving propagation modes in order to reduce selective fading. In addition, their use could provide marked reduction in interference to the extent that interference and desired signal do not coincide in vertical angle. Although both arrays were apparently successful in their objectives, published data are not sufficient to determine whether or not the ionosphere actually could support the theoretical vertical resolutions of these arrays.

A particularly important experiment relative to the feasibility of very large broadside arrays was performed by Balser and Smith [Ref. 15]. They studied a 1600 km north-south path and transmitted 35 μsec Gaussian pulses in order to separate and identify modes. Received amplitudes were measured at six whip antennas nonuniformly spaced along a line perpendicular to the direction of propagation. The distance between end elements was 2000 ft. In calculating the amplitude correlation between elements, the principal result was that the

correlation distances were much greater than expected. Correlation distance, in this case, was defined as the spacing between two elements which would reduce the correlation coefficient to 0.5. Of 31 cases studied, only seven had correlation distances of less than 2000 ft. The remainder had to be estimated by extrapolation, and in five cases this led to an estimate of 10,000 ft or more for the correlation distance. Most of the single-hop modes produced correlation distances of about 40 wavelengths, leading to an estimate of the angular fluctuations of the arriving signals on the order of 0.2 deg. Multiple-hop paths had correlation distances of around 10 wavelengths, implying angular fluctuations of about 1 deg.

While this experiment did not directly measure the all-important distributions of phase across the aperture which are needed to completely evaluate the performance of a phased array, the results are important in that they indicate the extent to which wavefronts may be essentially linear.

A more conclusive experiment which was performed by the author is directly applicable to predicting the performance of a very large array. This work has been described elsewhere [Refs. 16, 17] and will be only briefly reviewed here. CW signals propagated over a 2600 km east-west path were received at eight vertical whip antennas uniformly spaced 360 m apart along a north-south line. The total array was therefore 2520 m long. (This array actually constituted eight initial elements for the large receiving array which will be described in the next chapter.) Using feedlines of equal length, a receiving system with eight channels matched in amplitude and phase, and conventional phase meters, the distributions of amplitude and phase across the array were measured for received signals.

Because of equipment limitations, reception was limited to CW signals. Consequently, in order to eliminate interference between modes, frequencies propagating only a single mode were selected on the basis of oblique soundings. This circumstance limited the study exclusively to one-hop F2 low ray during quiet daytime conditions, since this ray provides the only essentially single-mode propagation which is possible over the path.

The experiment showed that for periods of several minutes the amplitude and phase distributions were quite linear across the array. The periods themselves were limited in extent by deep amplitude fades which were believed to result from polarization rotation with time. The predominant observed effect was a slow drift in the apparent transmitter bearing, which was confined to within ± 0.25 deg of the true bearing. The conclusion was that significant periods of time exist when the full performance (ideal pattern) of a 2.5 km array can be realized in receiving one-hop F2 low ray.

C. APPROACH USED IN THE PRESENT STUDY

While it had been shown that a large broadside array can sometimes perform well when receiving one-hop F2 low ray during quiet daytime conditions, it remained to show how well such an array would perform for other modes and under a variety of propagation conditions. In view of this, a 2.5 km broadside receiving array has been constructed and used to study the azimuthal properties of signals propagated over a 2600 km oblique path. The array is filled (elements are spaced less than a wavelength apart) in order to provide high directive gain and to eliminate ambiguities in azimuth (grating lobes).

The author supervised the design and construction of this array and did much of the design himself. It includes a number of novel features and represents a highly unusual facility in both scale and design. While the facility itself and the precision with which it was built are of great interest, the present work deals primarily with the array's performance as related to the properties of ionospheric propagation. A new technique for feedline matching, which was invented by the author and which proved to be of great importance in implementing the array, is described in the Appendix.

Throughout this work great emphasis has been placed on resolving and identifying propagation modes so that their individual azimuthal characteristics could be studied. To accomplish this, extensive use has been made of the sweep-frequency CW (SFCW) sounding technique. This

technique has been available for HF research only in recent years and will be discussed in some detail in the next chapter.

In addition to conventional techniques of array processing, this research has made extensive use of new digital processing techniques. Digital techniques have permitted significant improvements in the precision and flexibility of measurements.

Figure 1 Photograph of the 256-element, 2.5 km receiving array located near Los Banos, California. The main data-processing van is visible in the distance at the left.

II. EXPERIMENTAL FACILITIES AND TECHNIQUES

The measurements described in this report were made using sweep-frequency CW (SFCW) sounding over a 2600 km east-west path between Bearden, Arkansas and Los Banos, California. This chapter describes briefly the Los Banos receiving site, the Bearden transmitting site, and reviews quickly the SFCW technique used extensively throughout this research.

A. RECEIVING SITE

The Los Banos, California receiving site, shown in Fig. 1, consists of a 256-element broadside array of 18 ft vertical whip antennas. The elements are spaced 10 m apart along a north-south line, providing a total aperture of 2550 m. A ground mat 72 ft wide by 8500 ft long having a 2 ft mesh is provided to stabilize element impedance.

The main beam of the array may be electrically slewed in 0.25 deg steps ± 16 deg from the array boresite direction of true east. Slewing is accomplished by reed relay switches which add coaxial cable delay lines in series with the coaxial cable feed-lines of the array. The array incorporates a modified "Dolph" amplitude taper [Ref. 18] which provides sidelobes at least 20 dB below the main lobe, and half-power beamwidths of 0.25 deg at 29 MHz and 0.5 deg at 14.5 MHz. Table 1 lists 3 dB, 6 dB, 10 dB and 20 dB beamwidths versus frequency for the array.

The array is organized into 8 subarrays as illustrated by Fig. 2. In each subarray the outputs of 32 adjacent elements are fed through equal-length coaxial feedlines 540 ft long to an underground equipment room (bunker) where they are combined and time-delay steered into a single output. The 8 subarray outputs are then amplified and fed through equal-length feedlines 4300 ft long to the main processing van, where they may be processed separately or combined and steered into a single output. All feedlines are 0.5 in. foam-dielectric coaxial cable

TABLE 1

THEORETICAL 3 DB, 6 DB, 10 DB and 20 DB BEAMWIDTHS VERSUS FREQUENCY OF THE LOS BANOS RECEIVING ARRAY

FREQUENCY	BEAMWIDTH (deg)			
MHZ	3 DB	6 DB	10 DB	20 DB
1	7,26861	10,0352	12,5252	16,1371
2	3,63247	5,01278	6,25324	8,04852
3	2,42143	3,34126	4,16768	5,36323
4	1,81601	2,50579	3,12546	4,02178
5	1,45279	2,00458	2,50025	3,21718
6	1,21065	1,67045	2,08334	2,68088
7	1,03769	1,4318	1,78583	2,29784
8	,907976	1,25282	1,56258	2,01058
9	,807088	1,11361	1,38895	1,78716
10	,726378	1,00225	1,25005	1,60843
11	,660343	,911134	1,13641	1,4622
12	,6053.4	,835205	1,0417	1,34035
13	,558751	,770957	,961571	1,23724
14	,51884	,715888	,892886	1,14886
15	,48425	,668162	,833359	1,07227
16	,453985	,626401	,781273	1,00525
17	,427279	,589554	,735316	,946117
18	,403542	,556801	,694464	,893554
19	,382303	,527495	,657913	,846524
20	,363187	,50112	,625017	,804197
21	,345893	,477257	,595254	,765901
22	,33017	,455563	,568197	,731087
23	,315815	,435756	,543492	,6993
24	,302656	,4176	,520847	,670163
25	,29055	,400896	,500013	,643356
26	,279375	,385477	,480761	,618611
27	,269027	,3712	,462975	,595699
28	,259419	,357942	,44644	,574424
29	,250474	,3456	,431045	,554616
30	,242125	,33408	,416877	,536129
31	,234314	,323303	,403236	,518834
32	,226992	,3132	,390635	,502621
33	,220113	,303708	,378797	,48739
34	,213639	,294776	,367656	,473055
35	,207535	,286354	,357151	,459539
36	,20177	,278399	,347231	,446774
37	,196317	,270875	,337845	,434699
38	,191151	,263747	,328955	,423259
39	,18625	,256984	,32052	,412406
40	,181593	,250559	,312507	,402096

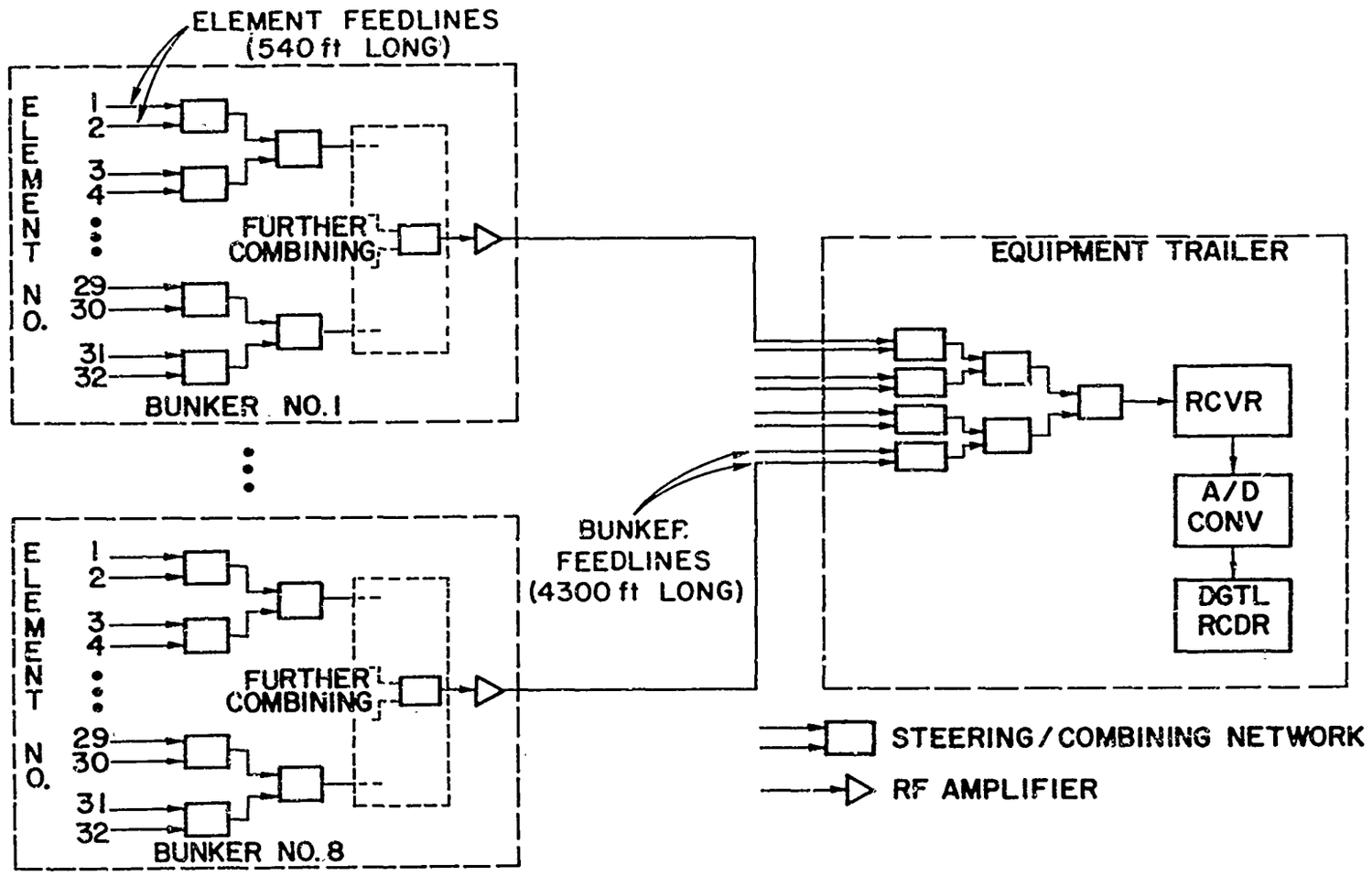

Figure 2 Block diagram of the beam-forming system for the receiving array.

(type RG-331/U) buried 4 ft beneath the ground for temperature stability.

In addition to the alternative of operating with the full array or with eight subarrays, a switch is provided which enables the received wavefronts to be sampled at only eight points across the aperture. In this mode an element of each subarray is fed through the bunker amplifier and feedline to the main processing van. This provides an array of eight whips uniformly spaced by 360 m across an aperture of 2520 m.

One of the most difficult problems in implementing the Los Banos array involved finding a technique which would allow the feedlines in the system to be matched in length with sufficient accuracy. The solution to this problem came with the invention by the author of a new technique of feedline matching which combines excellent accuracy with exceptional convenience [Ref. 19]. This technique is described in detail in the Appendix.

B. TRANSMITTING SITE

The Bearden, Arkansas, transmitting site is located east of the Los Banos receiving site at a range of 2600 km. The great-circle path connecting the two sites is perpendicular to the line through the receiving array elements.

The Arkansas site includes a sweep-frequency CW (SFCW) generator; broadband, linear, HF amplifiers providing output power up to 1 kW; a rotatable horizontal log-periodic antenna (LPA) on a 100 ft tower (Collins 237B-3); a frequency standard; and a programmed timer for synchronization purposes.

C. SWEEP-FREQUENCY CW (SFCW) SOUNDING

The principle involved in SFCW sounding is quite simple. If a sinusoidal signal whose instantaneous frequency is changing linearly with time is propagated through a fixed time delay, the length of delay

can be determined by measuring the frequency difference between the signals at the input and output of the delay. That is,

$$\tau = \frac{\Delta f}{s} \tag{2.1}$$

where

τ is the unknown time delay (sec)

Δf is the difference between input and output frequencies (Hz)

s is the rate of change of transmitted frequency with time (df/dt), also called the sweep rate (Hz/sec)

This assumes, of course, that s and τ are both constant with time. Note that if τ is a function of frequency (dispersive in nature) then Δf will vary with frequency also, and measurement of τ will be more complicated but, in general, possible. If τ varies with time, however, a change in frequency (doppler shift) will be imposed upon the signal which will cause an erroneous measure of τ at any instant. Fortunately, for the purposes of the work described here, time delays vary slowly enough with time that the doppler shifts introduced may be assumed negligible.

The SFCW technique may be used for ionospheric sounding to produce ionograms (plots of propagation time delay versus transmitted frequency). A signal is transmitted whose frequency is swept linearly with time over the frequency band of interest, and the difference frequency between the transmitted and received signals is measured to determine time delay, as explained above. Since the signal can propagate simultaneously via several ionospheric modes having different time delays, several frequency differences must be measured simultaneously. This can be done with various techniques of spectrum analysis and, in practice, certain commercially available spectrum analyzers are quite satisfactory for this purpose.

Figure 3 shows a block diagram of a sweep-frequency sounding system. For transmitting, the output of the sweep-frequency generator is amplified and fed to an antenna. Since the receiver may be thousands of kilometers from the transmitter, it is not in general possible to have the actual transmitted waveform available at the receiver to compare with the received signal. Consequently another sweep-frequency generator is used at the receiver to generate a local equivalent of the transmitted signal, shifted up by an amount equal to a convenient system intermediate frequency (IF). This locally generated signal is then mixed with the received signal and the difference frequencies are selected by a single-sideband (SSB) receiver which is permanently tuned to the system IF frequency. The receiver and a product detector convert the difference frequencies to audio frequencies, where their spectrum is analyzed and recorded as a function of time on facsimile paper with signal amplitude displayed as intensity. Since the transmitted frequency is linearly increasing with time, the resulting display of audio spectrum versus time is also a display of time delay (from transmitter to receiver) versus transmitted frequency. The latter display is commonly called an ionogram. To insure proper timing, sweeps are initiated by programmed timers which are synchronized to accurate time standards such as signals from station WWV or cesium clocks, depending upon the accuracy required.

Sweep-frequency CW sounders typically sweep 3 MHz to 30 MHz. Generating sweeps of sufficient linearity for this application became practical only after the advent of fast frequency-stepping, programmable frequency synthesizers. Modern linear-sweep generators consist of such synthesizers digitally programmed to step the frequency rapidly in small increments (typically steps of 1 Hz) in order to generate a stepwise approximation to a linear ramp. Details of this procedure plus performance specifications can be found elsewhere. [Ref. 20]

From Eq. (2.1), the time-delay resolution of an SFCW sounder is a function of the sweep rate and the resolution of the spectrum analyzer. For most of the work reported here a sweep rate of 250 kHz/sec and an analyzer resolution of 2 Hz were used to provide a time-delay resolution of 8 μsec.

Compared to pulse sounders, SFCW sounders offer excellent immunity to interference from other users of the HF spectrum. This is because the apparent frequencies of the interfering stations are changing so rapidly at the input to the spectrum analyzer that they remain in an individual analyzer filter for only a very small fraction of its rise time. In addition, since the SFCW sounder sweeps continuously through the spectrum with a comparatively narrow bandwidth receiver, it makes maximum use of the clear frequencies between interfering stations.

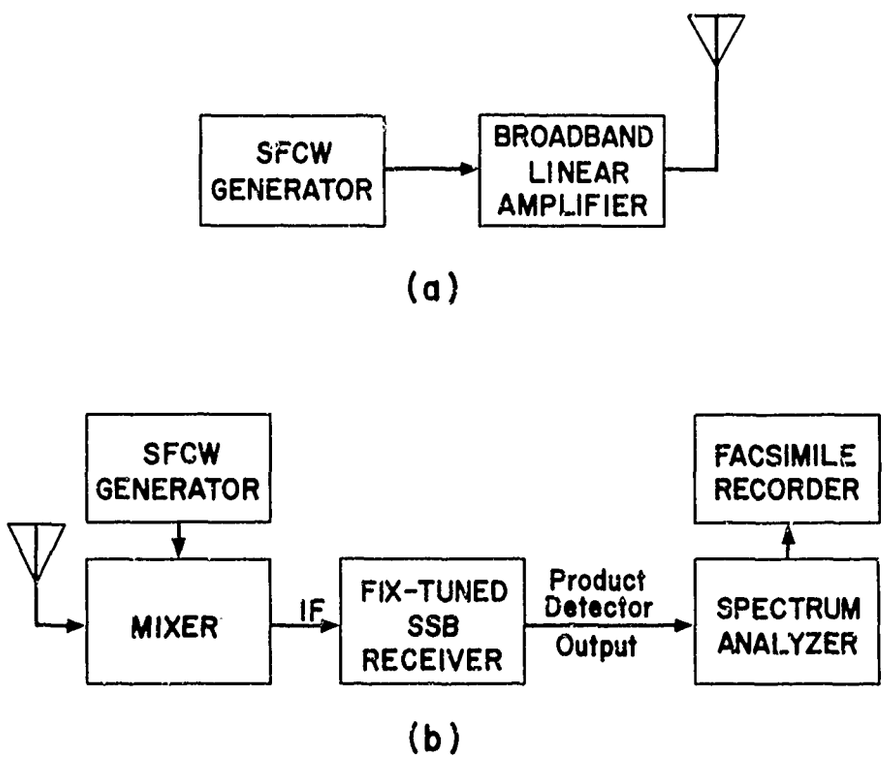

Figure 3 Block diagram of a sweep-frequency CW (SFCW) sounder.
(a) Transmitter.
(b) Receiver.

III. LOW-POWER OBLIQUE SOUNDINGS

The exceptional immunity to interference and to directional noise conferred by the combination of linear SFCW signals with a large-aperture HF array, has made possible the use of extremely low powers in oblique ionospheric sounding. Usable midday ionograms over a 2600 km east-west path have been obtained with transmitter powers as low as 50 μW. With such low transmitted power, interference to distant users of the HF spectrum is virtually eliminated, and interference to local users is also greatly reduced.

Examples showing the dependence of sounding quality upon receiving array directivity, array slewing, and transmitted power are presented below. These will illustrate the unprecedented sensitivity of the sounding system and will demonstrate for the first time the ability of a system to carry out useful ionospheric research with less than 5 mW of radiated power.

A. EXPERIMENTAL DESIGN

The soundings now to be described were made over the 2600 km east-west Bearden-to-Los Banos path using the system discussed in Chapter II. Signals were transmitted from the Arkansas site by feeding the 50 mW output of the sweep-frequency synthesizer through an attenuator to a Collins 237B-3 LPA directed toward the Los Banos receiving array. In each case a sweep rate of 250 kHz/sec was used. Received signals were deramped in the usual fashion and spectrum-analyzed to an effective audio frequency resolution of 2 Hz, thus providing an averaging time of about 1/2 sec and a range resolution of 8 μsec.

B. EXPERIMENTAL RESULTS

Examples of ionograms generated with transmitted powers ranging from 50 mW to 50 μW are shown in Fig. 4. At approximately 0800 midpath time, these records were produced at 2 min intervals in order of

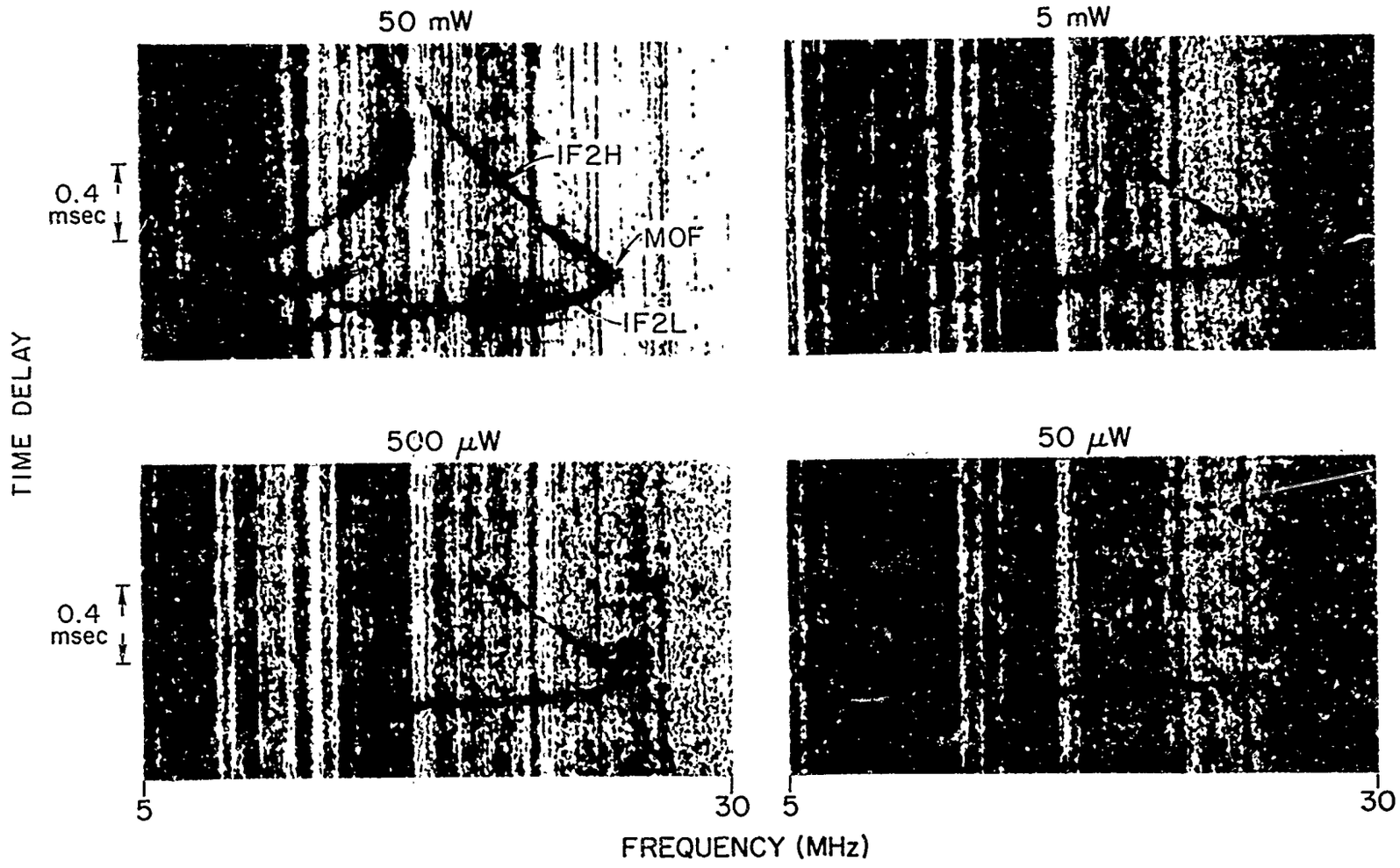

Figure 4 Low-power Bearden-to-Los Banos oblique soundings made on 26 Sept 1968 at about 1500 UT (0800 midpath time) using the full 256-element receiving array.

decreasing power. Signals were swept from 5 MHz to 30 MHz at a 250 kHz/sec rate, requiring 1 min 40 sec to produce each record. Using all 256 elements, the receiving array was steered to a bearing of 90 deg--the true transmitter bearing. The dark vertical bars on the records were caused by interfering stations. Notice that with only 50 μW of transmitted power, one-hop F2 low ray (1F2L), high ray (1F2H), and the Maximum Observed Frequency (MOF) can still be seen. For comparison, certain FCC Citizen Band requirements allow unlicensed operation with input powers of 100 mW, giving an effective radiated power (ERP) probably 20 dB higher than that used here.

The dependence of sounding quality upon the directive gain of the receiving antenna is illustrated by Fig. 5. Here records were produced two minutes apart with a transmitted power of 5 mW using the full array of 256 elements, a subarray of 32 elements (one-eighth of the full aperture), and a single element of the array. The gain of the full array with respect to a single element is about 24 dB; and the gain of a subarray with respect to a single element is about 15 dB. For comparison, a subarray record taken with power reduced by 10 dB is shown. Notice for the one-hop F2 low ray (1F2L) that the received signal strength is clearly greater for the full array than for a subarray or a single element. This illustrates qualitatively that the directive gain of the 2.5 km array can be beneficial for receiving ionospherically propagated signals. The 5 mW record taken with a single vertical whip illustrates the great immunity to interference and noise afforded by the linear SFCW technique.

When the number of elements is reduced from 256 to 32 in Fig. 5, the increase in signal strength of the high ray (1F2H) is caused by the fact that its angle of arrival lies outside of the nominal 0.25 deg beamwidth of the 256-element array, but inside the nominal 2 deg beamwidth of the 32-element array. This effect is illustrated more clearly by Fig. 6. In producing this sequence the transmitted power was 5 mW, and the full 256-element array was steered in azimuth from 89.5 deg to 92.0 deg in 0.5 deg steps. During these tests the array had a uniform amplitude taper, rather than the "Dolph" taper, so that its pattern was

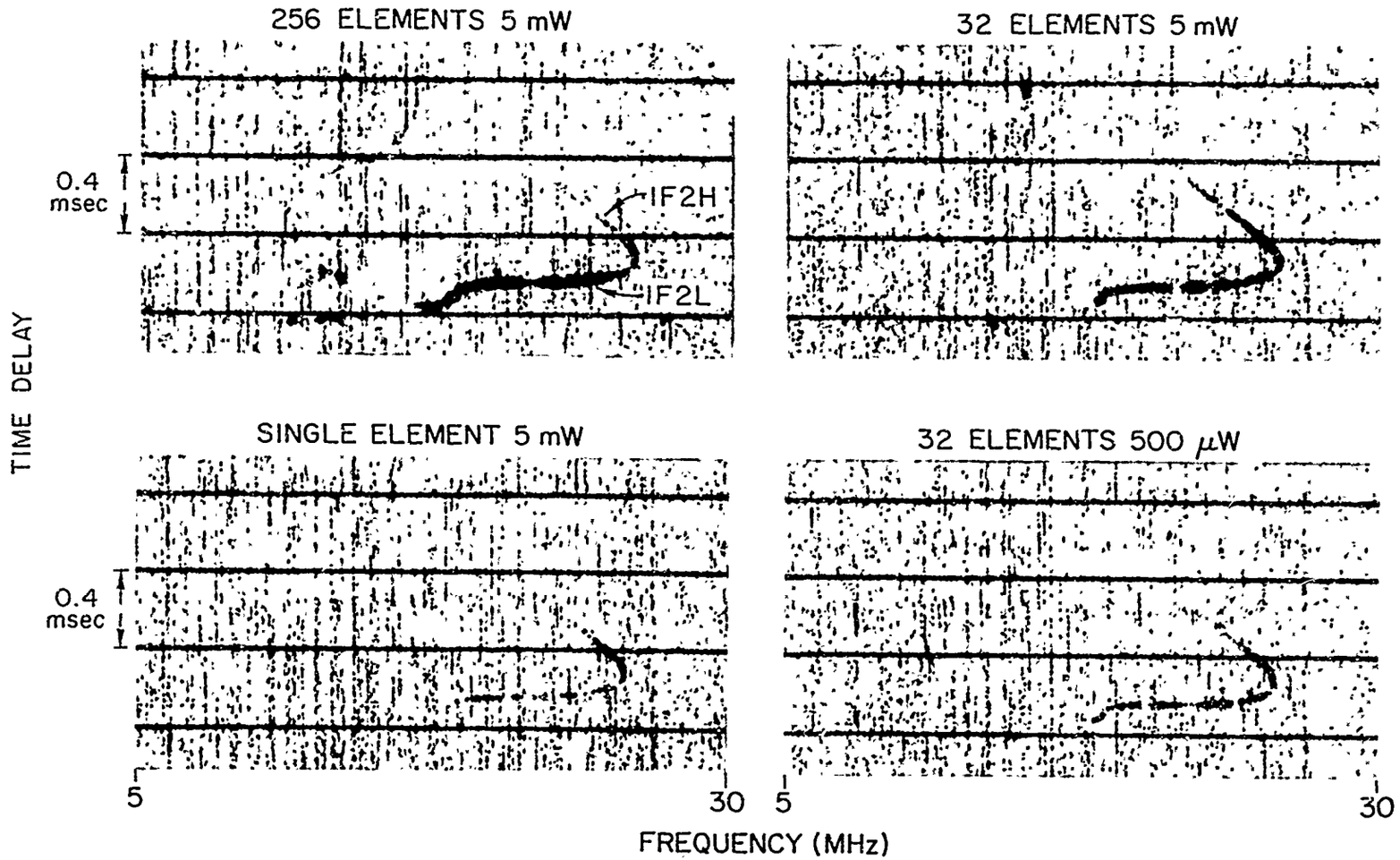

Figure 5 Low-power oblique soundings made on 3 Oct 1968 at about 1640 UT (0940 midpath time) showing the dependence of record quality upon the directive gain of the antenna.

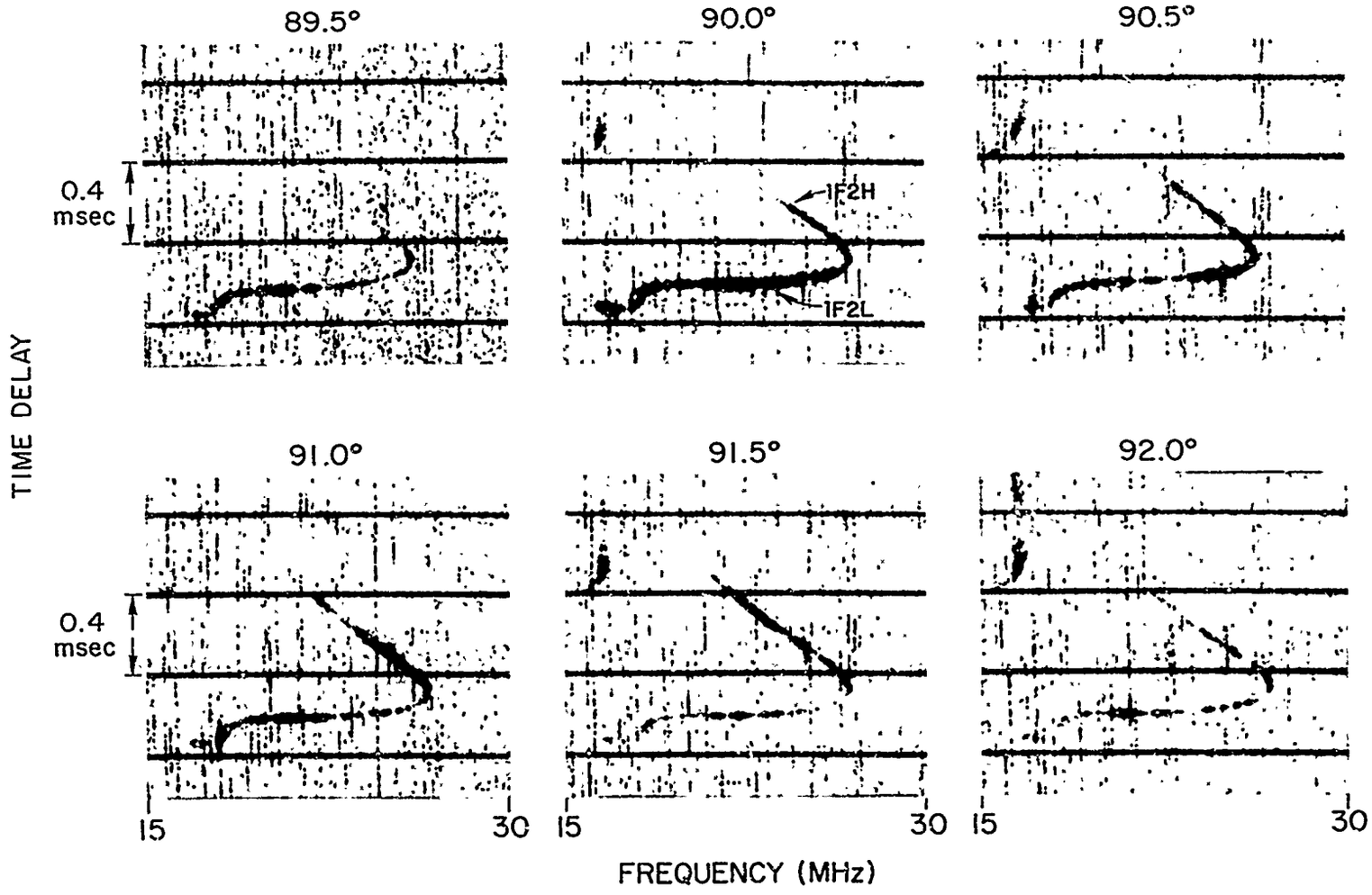

Figure 6 Low-power (5 mW) soundings made on 3 Oct 1968 at about 1700 UT (1000 midpath time) showing the dependence of record character upon the main lobe direction of the 256-element array.

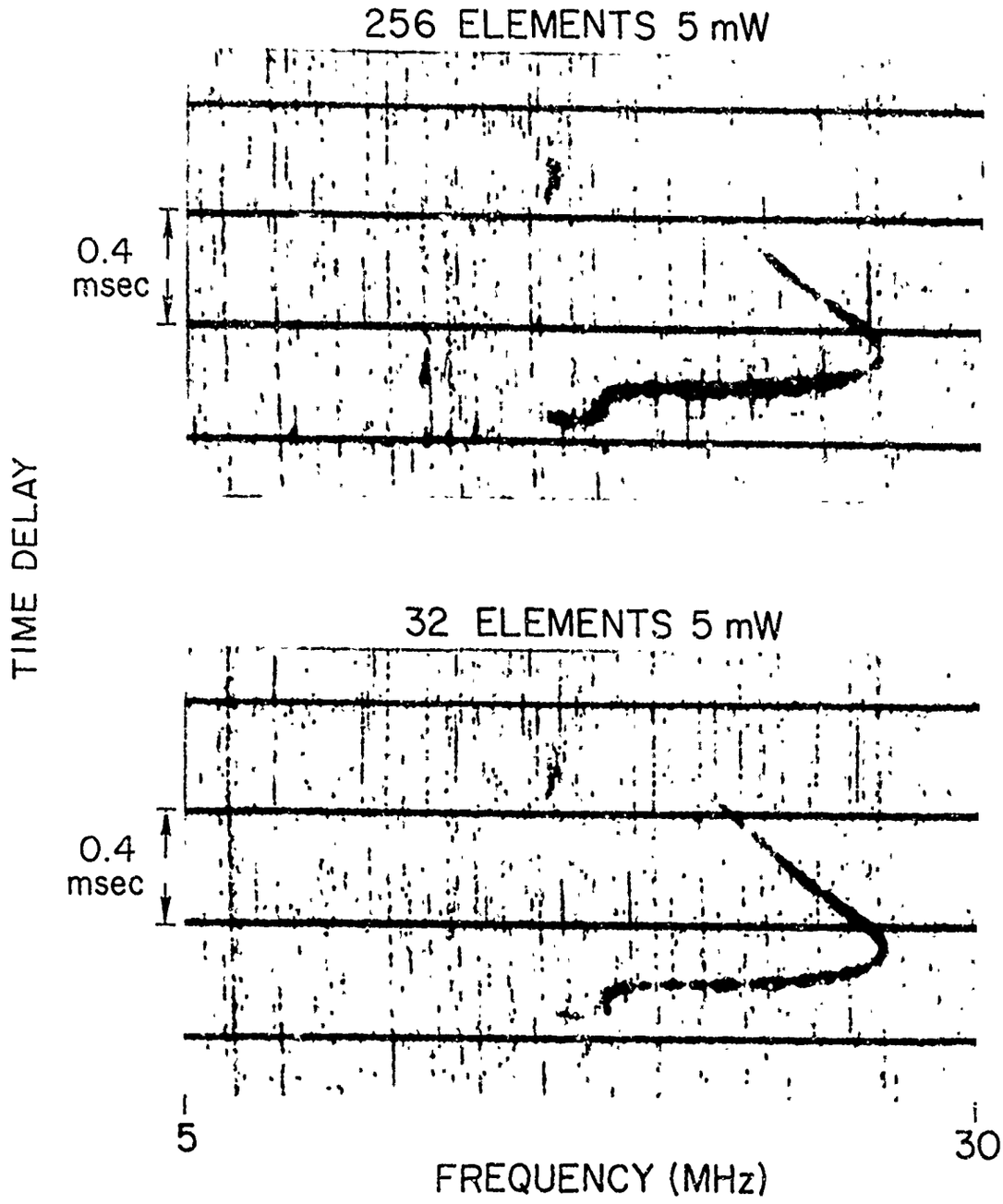

Figure 7 Low-power soundings made on 3 Oct 1968 at about 1700 UT (1000 midpath time) illustrating the change in record character produced by broadening the antenna beamwidth.

the familiar (sin x)/x array pattern. As a result, a point source could be received in an attenuated fashion even when it was not in the main lobe. Soundings were made every two minutes, and each alternate sounding was made with the array steered to 90 deg to look for variations of the ionograms with time. Since no significant changes occurred at 90 deg during the sequence, the differences in the records shown in Fig. 6 can be attributed to changes in azimuth rather than to changes of ionospheric conditions with time.

The most interesting feature of these records is the relative intensities of the low and high rays. At 89.5 deg the low ray was decidedly stronger than the high ray. At 90.0 deg the low ray was stronger than at any other steering angle and the high ray was still much weaker. In going from 90.0 deg to 90.5 deg the low ray decreased and the high ray increased in intensity. At 91.0 deg the strength of the high ray increased even further, and high and low rays were of approximately equal magnitude. At 91.5 deg the high ray was clearly stronger than the rather weak low ray. It appears that the low ray was strongest at a bearing of 90 deg, and the high ray was strongest between 91.0 deg and 91.5 deg. From this observation it can be concluded that the low ray was arriving from the true transmitter bearing, and that the high ray was arriving from an azimuth about 1.25 deg south of the true bearing.

The fact that the high ray and the low ray may have angles of arrival differing by more than one degree explains why changing from the full array to a subarray (increasing the beamwidth from 0.25 deg to 2 deg) can make the amplitudes of the two rays more nearly equal. Figure 7 shows an excellent example of this. In the upper ionogram, which was taken with the full array, the lower ray is clearly stronger than the upper ray. In the lower ionogram, which was taken two minutes later with a subarray, the upper and lower rays are of nearly equal strength.

Additional observations of and an explanation for the southerly deviation of the high ray will be presented in the next chapter.

IV. AZIMUTHAL DISTRIBUTIONS OF IONOSPHERIC MODES

The performance of a highly directive antenna array depends upon the directional properties of the signals it receives. Measurements described in Chapter I of amplitude and phase across the 2.5 km Los Banos array indicated that one-hop F2 low ray, at least at times, exhibits a discrete azimuth. At these times, the full directive gain of the array can be realized for receiving this mode. Since those measurements required CW signals, they were limited to frequencies which propagated only a single mode in order to avoid multi-mode interference. This restricted study to the one-hop F2 low ray over a very limited frequency range during quiet daytime conditions.

This chapter will describe another experiment which measures directly, with angular resolution nearly an order of magnitude greater than any used previously, the azimuthal distributions versus time and frequency of a variety of other ionospheric modes in addition to the one-hop F2 low ray mode. This experiment has afforded several new insights into ionospheric propagation, which will also be discussed.

A. EXPERIMENTAL PROCEDURE

In this experiment SFCW signals were transmitted from Bearden, Arkansas, over the 2600-km east-west path to Los Banos, California, where they were received using the full amplitude-tapered, 256-element array described in Chapter II. SFCW soundings were taken frequently to aid in interpretation of data and identification of propagation modes. All records were taken with average and peak transmitter powers of less than 5 W.

Data were taken with the system illustrated in Fig. 8. SFCW, having a sweep rate of 250 kHz/sec and a bandwidth of 250 kHz, was transmitted every second from Arkansas, enabling the various ionospheric modes of propagation to be resolved in time delay. The 256-element receiving array was then stepped in azimuth by 0.25 deg each second, from 7 deg north to 7 deg south of the true transmitter bearing. The

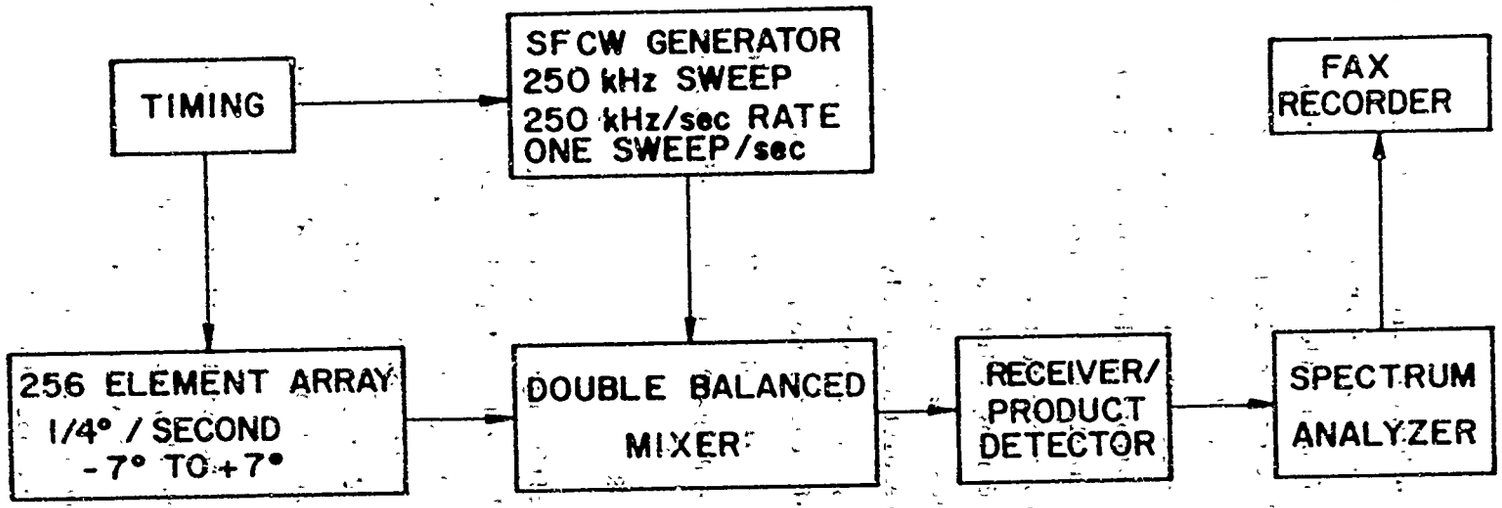

Figure 8 Block diagram of the system used to produce displays of time delay vs azimuth (azimuth scans).

received signal was deramped in the usual fashion, with the SFCW generator using a sweep rate of 250 kHz/sec and sweeping a single 250 kHz bandwidth every second in synchronism with the stepping of the array in azimuth. In this way, one full 250 kHz sweep was recorded at each array bearing. After detection and spectrum analysis, the facsimile recorder output produced a display of time delay vs azimuth, with received signal amplitude shown as "display intensity."

The start frequency (low-frequency limit) of the transmitted frequency sawtooth could be stepped automatically to enable study of a variety of propagation modes, or it could be held fixed to study the time variability of a particular mode structure of interest. Data taken using both of these methods of recording are presented below.

B. EXPERIMENTAL RESULTS

Mode-resolved angle of arrival displays (azimuth scans) for odd start frequencies from 9 to 31 MHz are shown in Fig. 9. To aid in mode interpretation, a Bearden-to-Los Banos ionogram taken shortly after these azimuth scans is shown in Fig. 10. One-hop F2 low ray (1F2L) and one-hop F2 high ray (1F2H) are clearly visible, as well as two-hop and three-hop F2 (2F2 and 3F2). The mode in the lower left-hand corner of Fig. 10 having the shortest group delay of all of the modes is interpreted as two-hop E (2E). One-hop E is not visible over this path because of horizon screening.

From azimuth scans such as those in Fig. 9 it can be deduced that propagation modes involving ground reflections are usually spread both in time delay and in azimuth, while propagation modes not having ground reflections are in general discrete in time delay and azimuth. It should be explained that because of the limited dynamic range of the facsimile display, it is often impossible to display all modes of interest without saturating the display intensity on some modes. Consequently, a mode having a discrete angle of arrival such as the one-hop F2 low ray is sometimes visible even when it is received in the side lobes of the array, which are at least 20 dB weaker than the array

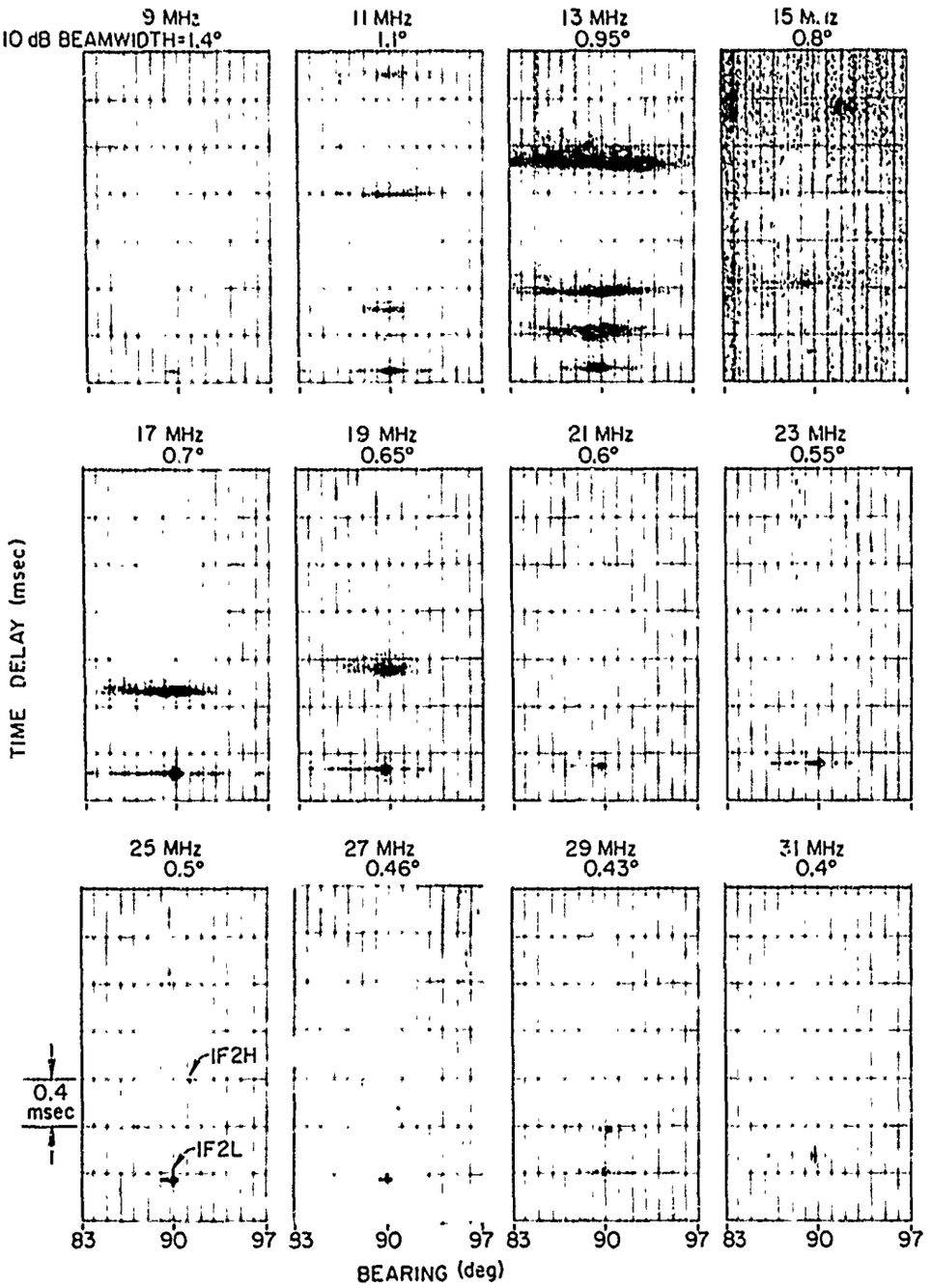

Figure 9 Displays of time delay vs azimuth (azimuth scans) at odd frequencies from 9 MHz to 31 MHz taken on 28 Mar 1969 at about 2230 UT (1530 midoath time). Beamwidths (10 dB) of the receiving array are listed to aid in interpretation. See Figure 10 for an ionogram taken at about this time.

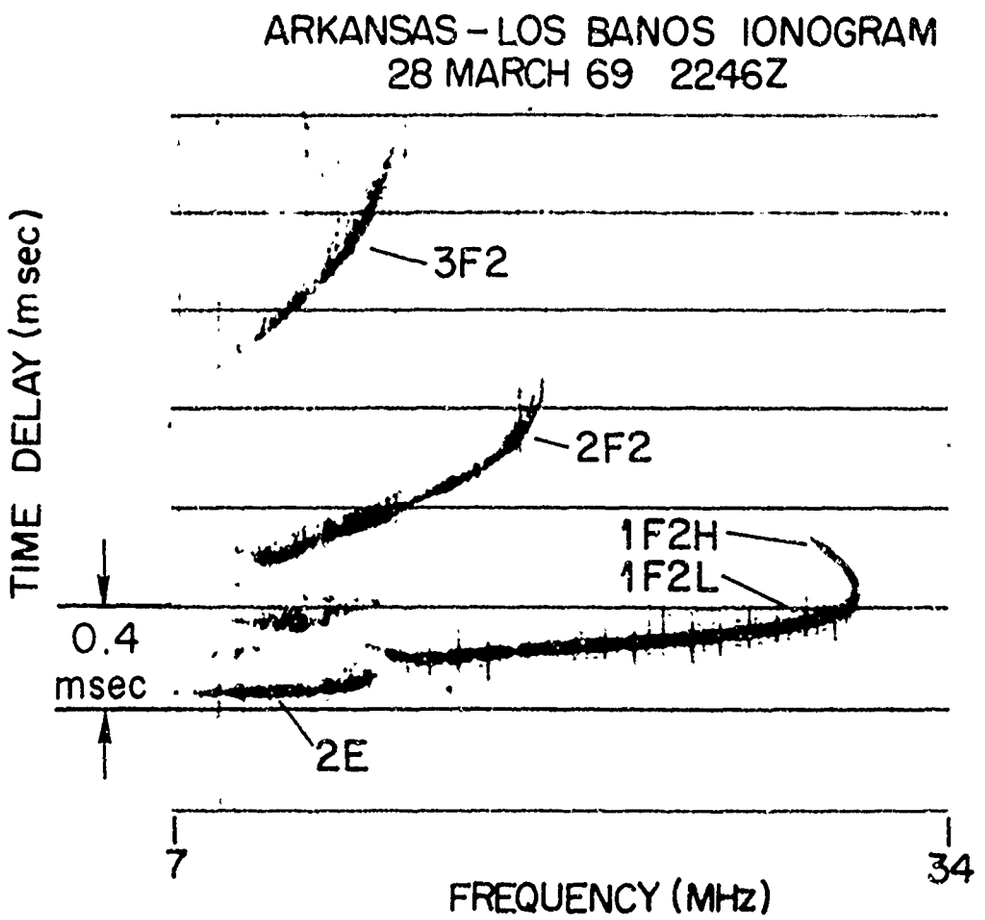

Figure 10 Ionogram taken 28 Mar 1969 at 2246 UT (1546 midpath time) to aid in interpretation of Figure 9.

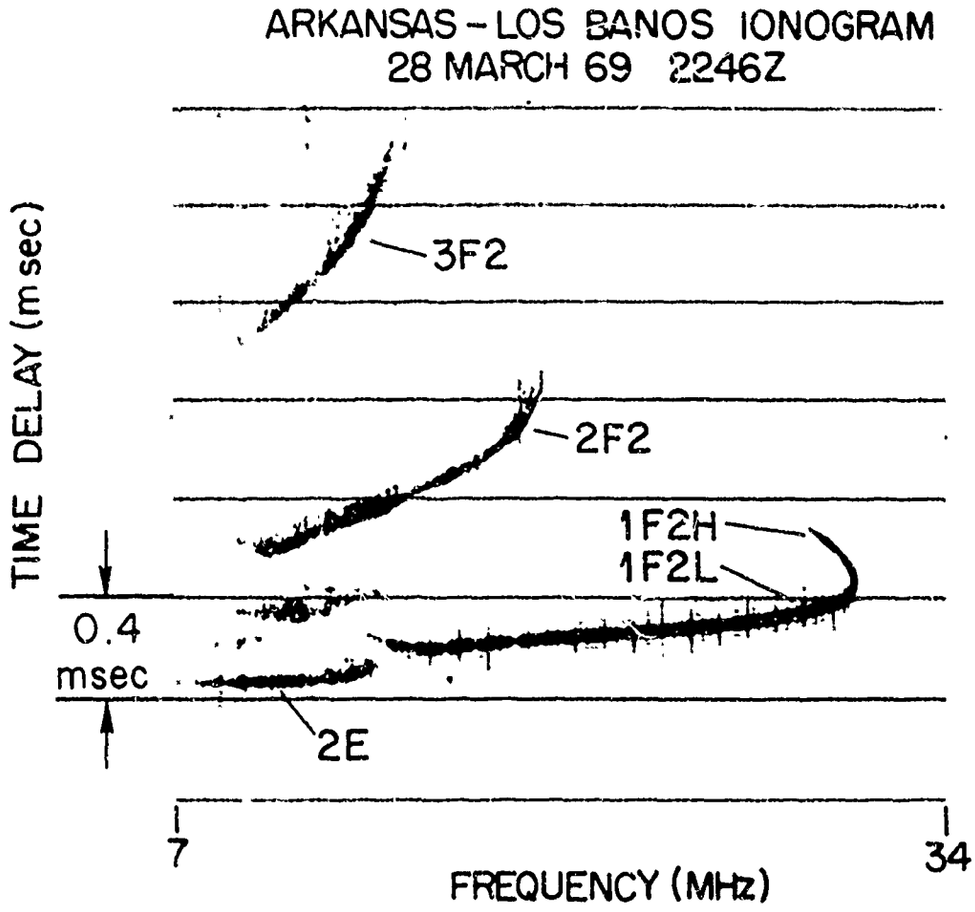

Figure 10 Ionogram taken 28 Mar 1969 at 2246 UT (1546 midpath time) to aid in interpretation of Figure 9.

main lobe. The discreteness of a mode can usually be deduced, however, from the increased width of the display trace as the main lobe of the array crosses the true angle of arrival of the mode.

As is demonstrated by the display at 25 MHz in Fig. 9, the one-hop F2 high ray can have an angle of arrival typically 1 deg to 1.5 deg south of the low ray. This effect, already mentioned in Chapter III, is quite common during quiet afternoon conditions, and will be explained in the next section. In addition, the angle of arrival of the one-hop F2 low ray during quiet conditions is nearly always within 0.5 deg, and usually within 0.25 deg, of the true transmitter bearing, just as in this example.

To illustrate the time variability of the angles of arrival of one-hop F2 low ray and one-hop F2 high ray during quiet summer conditions, azimuth scans at a fixed frequency were made for a period of about an hour on 25 August 1969, beginning at about 0300 midpath standard time. Figure 11 illustrates a Bearden-to-Los Banos ionogram taken just prior to these azimuth scans. Azimuth scans were made each minute at a frequency of 23 MHz, where both low and high rays were propagating. Figure 12 shows the angle of arrival of both the high and low rays vs time for a period of about an hour. Notice that the low ray is almost always confined to within 0.25 deg of the true transmitter bearing of 90 deg. The high ray varies everywhere from 1.25 deg south of the true transmitter bearing, to nearly the true transmitter bearing.

A similar sequence for disturbed summer conditions taken on 30 September 1969 at about 0100 midpath standard time is shown in Figs. 13 and 14. Figure 13, a Bearden-to-Los Banos ionogram taken just prior to this sequence of azimuth scans, shows the very complex mode structure that existed at the time. The F1 maximum frequency exceeded the F2. A sample azimuth scan taken at 14.5 MHz is also shown in Fig. 13. The most interesting feature of this record is that ordinary (O) and extraordinary (X) rays of the one-hop F2 high ray (which are resolved in time delay) exhibit slightly different angles of arrival.

Preceding page blank

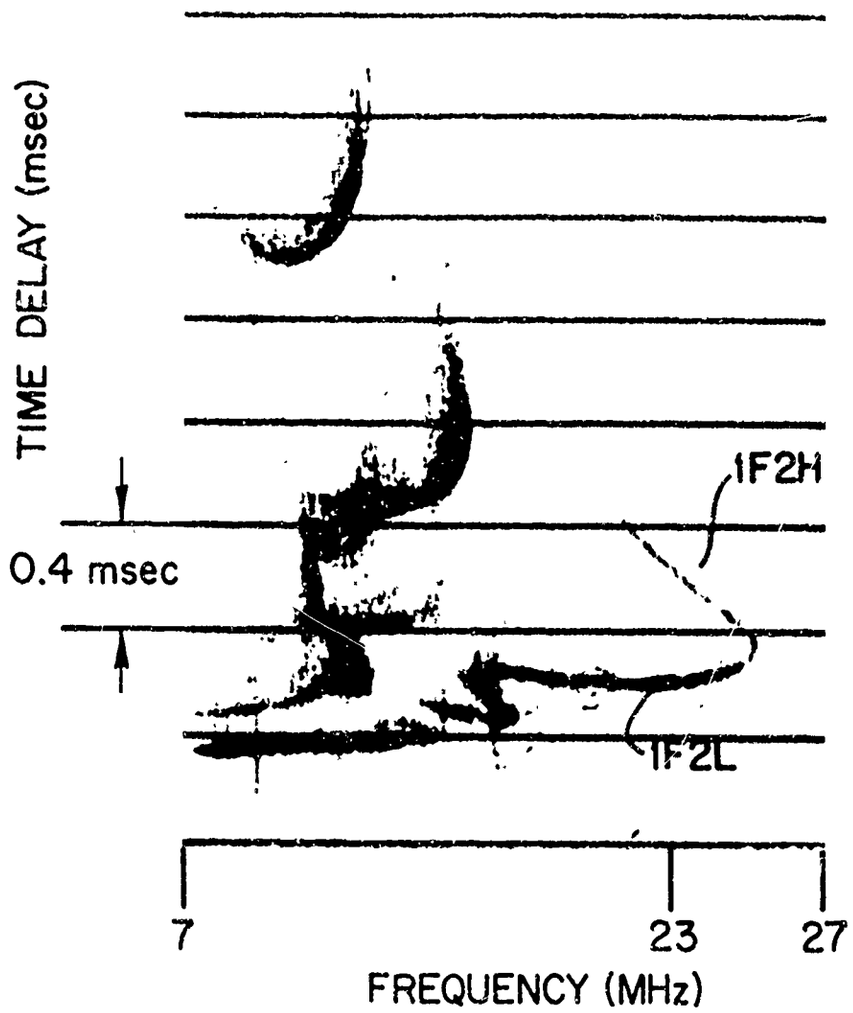

Figure 11 Ionogram taken 25 Aug 1969 at 2150 UT (1450 midpath time) just prior to the measurements plotted in Figure 12.

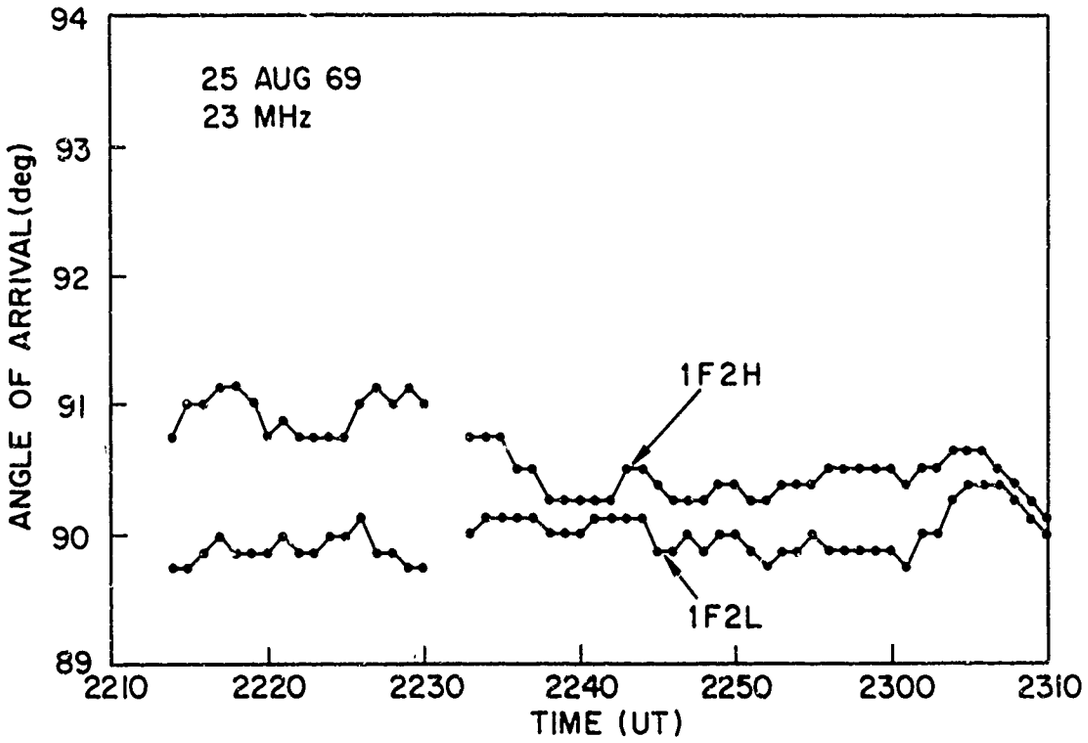

Figure 12 Plot of the angle of arrival vs time for the one-hop F2 low ray (1F2L) and the one-hop F2 high ray (1F2H) taken at 23 MHz on 25 Aug 1969. See Figure 11 for an ionogram taken at about this time.

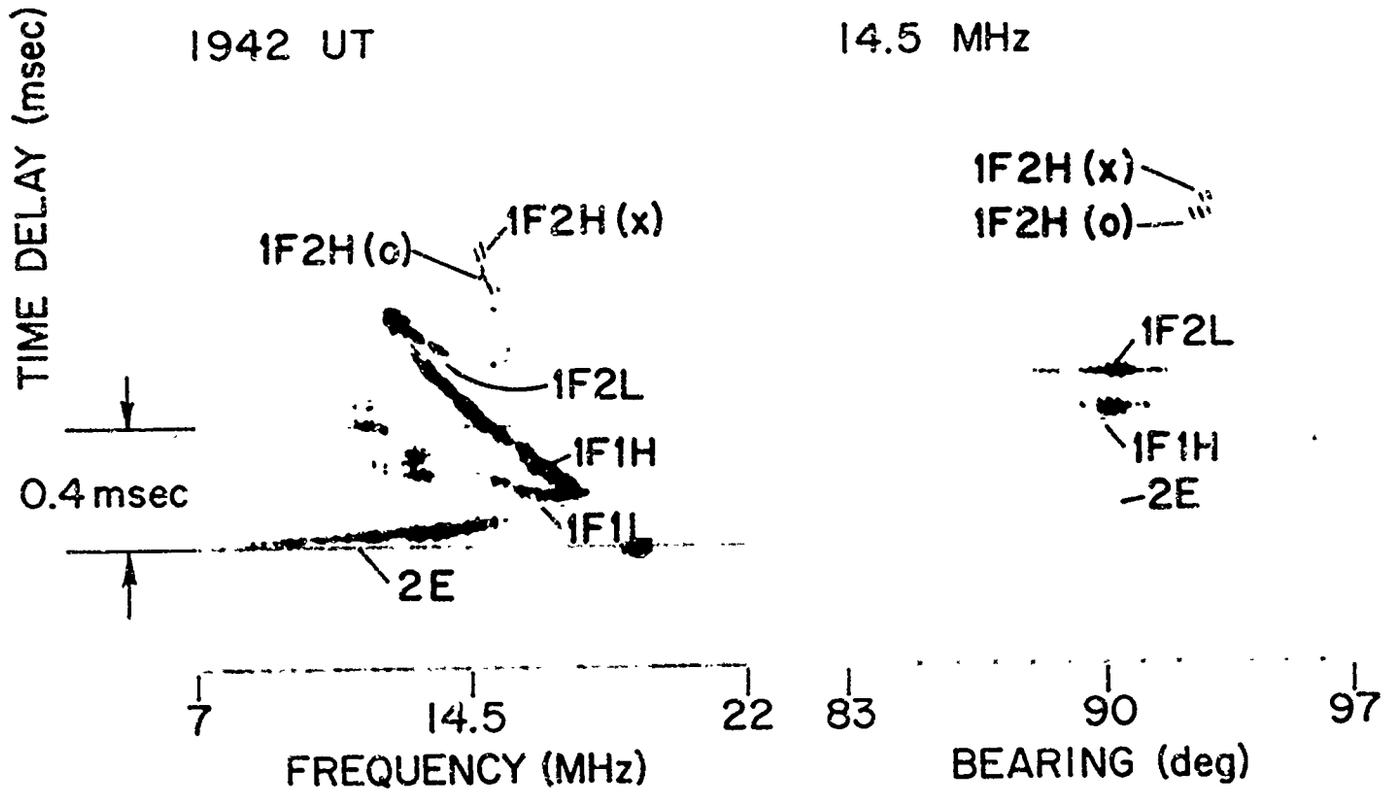

Figure 13 Arkansas-to-Los Banos ionogram (left) and azimuth scan at 14.5 MHz (right) taken 30 Sept 1969 at about 2000 UT (1300 midpath time).

Notice the different angles of arrival for the one-hop F2 high ray ordinary and extraordinary components [1F2H(o) and 1F2H(x) respectively].

Both rays are deviated nearly 3 deg south of the true transmitter bearing, and the extraordinary component is nearly 0.25 deg south of the ordinary component.

Figure 14 shows the angles of arrival vs time of all the modes propagating at 14.5 MHz. Notice that the deeper the mode penetrates into the ionosphere, the further south it is deviated from the true transmitter bearing, and the more variable is its angle of arrival.

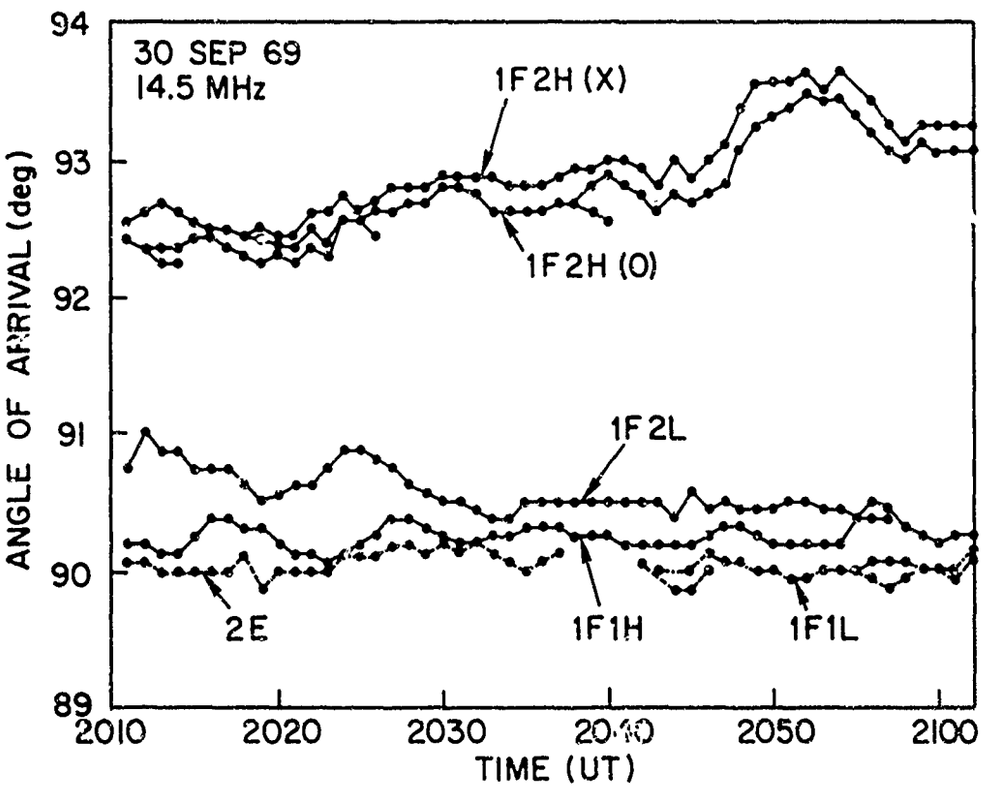

Figure 14 Angles of arrival vs time for the various ionospheric modes propagating at 14.5 MHz on 30 Sept 1969.

See Figure 13 for an ionogram taken at about this time.

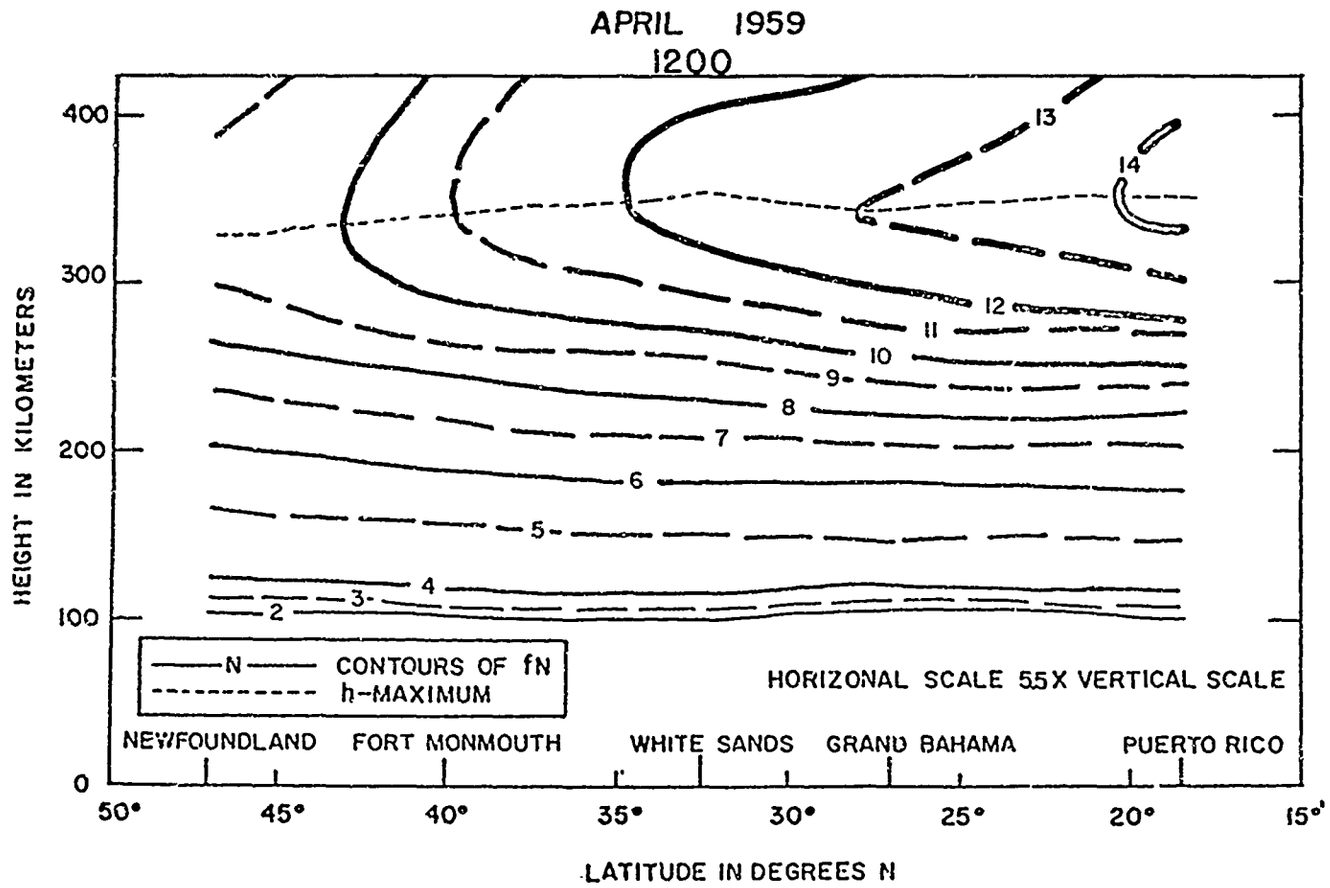

Figure 15 Plot of height vs latitude for contours of constant plasma frequency (constant electron density) derived from a monthly mean of local noontime measurements taken during April of 1959. (Taken from Ref. 21).

C. SOUTHERLY HIGH RAY DEVIATIONS

The frequent deviation of the high ray south of the low ray as described above can be understood by examining ionospheric profiles as a function of latitude during undisturbed daytime conditions. Figure 15 illustrates a height-vs-latitude plot for contours of constant plasma frequency f_N (constant electron density) as published in a National Bureau of Standards Technical Note [Ref. 21]. These true-height contours were estimated from measurements made by a north-south chain of vertical-incidence sounders, and represent a monthly mean of quiet conditions taken at noon local time during April of 1959. Notice that the contour lines slope upward with increasing latitude, and that the amount of slope increases with height at any given latitude. This suggests that the higher a ray penetrates into this particular ionosphere, the larger will be the effective ionospheric tilt that it experiences (an effect illustrated dramatically by Fig. 14). Since high rays penetrate the ionosphere more deeply than low rays at a given frequency, it would be expected that the high ray would be received with an angle of arrival south of the low ray.

To confirm this and to measure the amount of deviation that might be expected from a typical profile, the profile of Fig. 15 was modeled in a computer by a single Alpha-Chapman layer. The model used is illustrated in Fig. 16. Notice that, although there is no E layer present, the model ionosphere realistically incorporates the characteristic of increasing tilts with height in the F region.

Using the Jones three-dimensional raytracing program [Ref. 22] acquired from ESSA and adapted for use on a Stanford University computer, angles of arrival were measured for rays transmitted from a location corresponding to Bearden, Arkansas, and received in the vicinity of a location corresponding to Los Banos, California. The resulting plot is shown in Fig. 17, where angle of arrival vs range is plotted with frequency as a parameter. The rays which deviate farthest from the true transmitter bearing of 90 deg correspond to high rays,

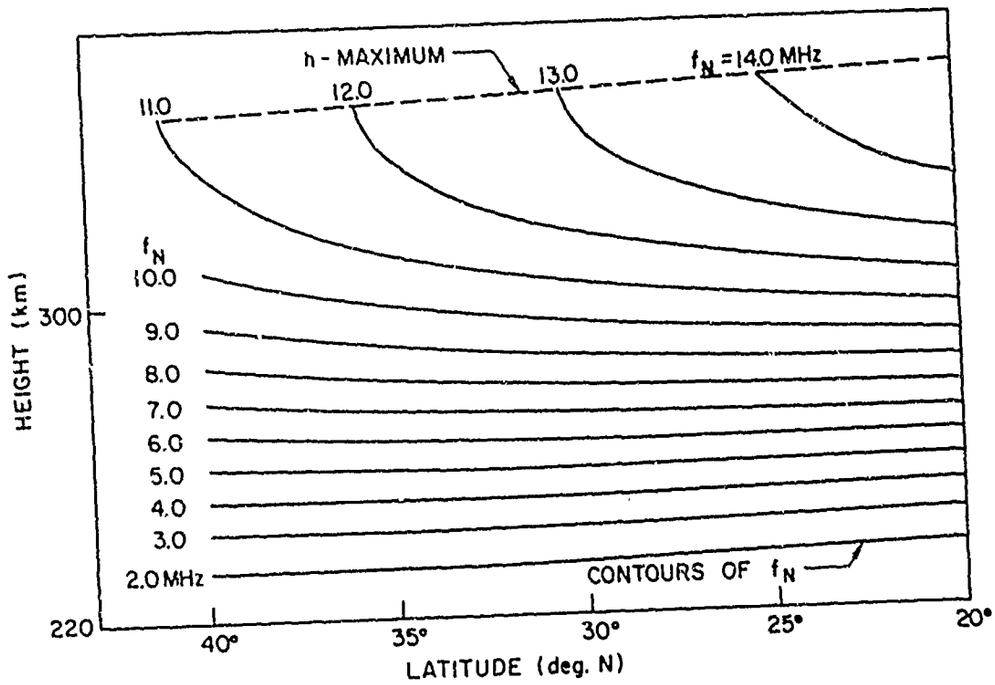

Figure 16 Computer model for ionosphere of Figure 15.

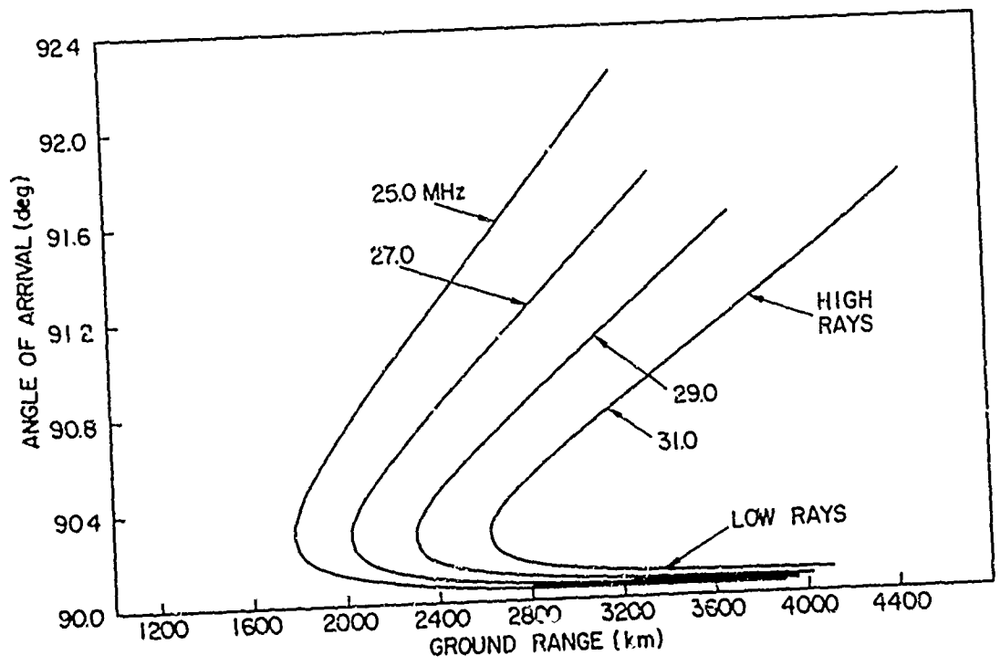

Figure 17 Plot of angle of arrival vs ground range, with frequency as a parameter, derived by three-dimensional computer raytracing using the model ionosphere of Figure 16.

and those which are close to the true transmitter bearing correspond to low rays. Note that at 25 MHz for the range of 2600 km (which corresponds to the distance between Bearden and Los Banos) the high ray arrives about 1.5 deg south, and the low ray by less than 0.1 deg south of the actual transmitter bearing. This result agrees well with the measured values shown in Fig. 9.

D. SUMMARY AND DISCUSSION

Mode-resolved measurements of the azimuthal distributions of ionospherically propagated radio waves have revealed the following:

(1) In a propagation mode that involves no ground reflections, the azimuthal distribution of received energy is usually discrete to within the azimuthal resolution of the 2.5 km receiving array. The performance of the receiving aperture does not seem to be seriously degraded by the reflection of signals from the ionosphere.

(2) The one-hop F2 high ray is often observed to have an angle of arrival south of the low ray (and the true transmitter bearing) by about a degree in azimuth. This can be explained by ionospheric tilts, which increase with height during the daytime. Such tilts were measured previously by NBS with vertical ionosondes, and the consistency between their measurements and the measurements described in this paper has been verified with three-dimensional raytracing by computer. This suggests a new technique for measuring ionospheric tilts vs height using oblique rather than vertical sounders.

(3) Whenever a propagation mode involves reflections from the ground, the received signals are generally spread both in time delay and in azimuth. The observed spreading of ground reflected signals is probably a consequence of the midpath reflection for this particular path occurring in the Rocky Mountains, an unusually rough scattering region.

(4) During quiet daytime conditions, the one-hop F2 low ray has an angle of arrival confined to within 0.5 deg of the true transmitter bearing, and usually lies within 0.25 deg thereof.

(5) In general, for afternoon conditions, the higher a ray penetrates into the ionosphere the more its angle of arrival will deviate from the true transmitter bearing, and the more it will vary with time.

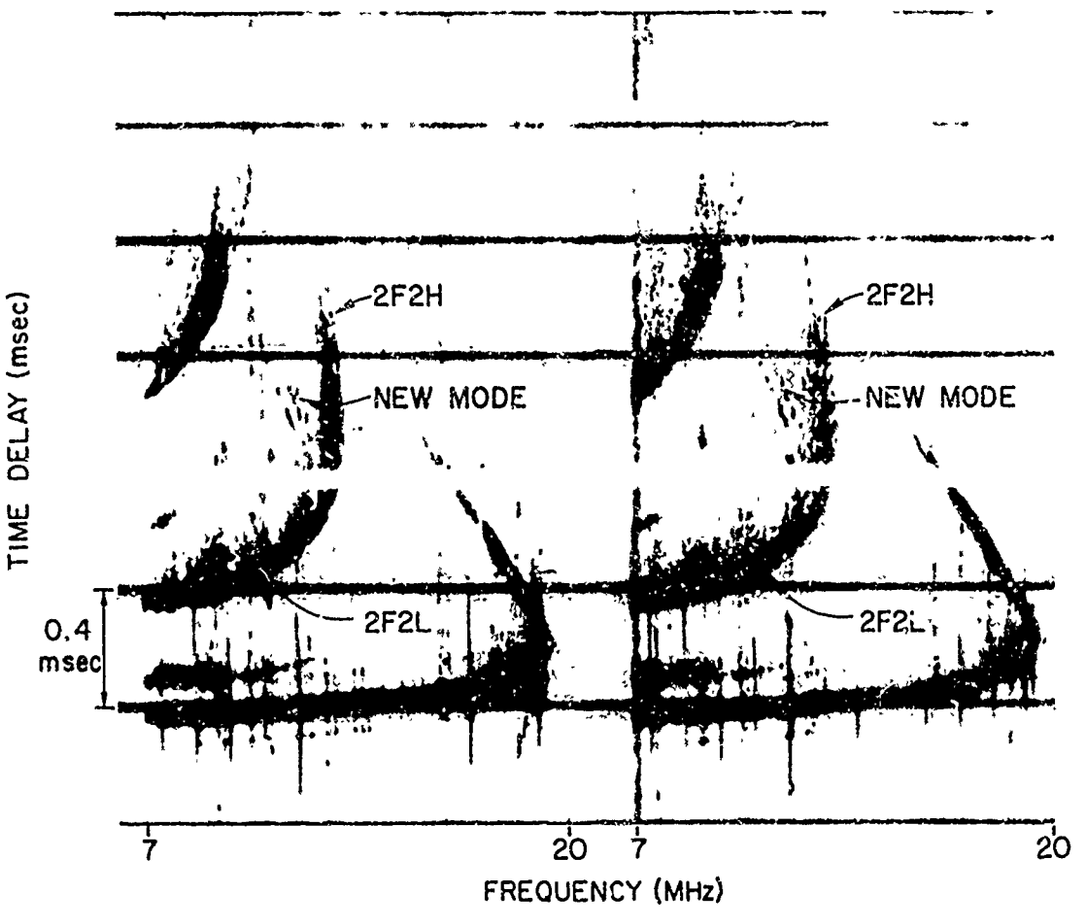

Figure 18 Ionograms taken 2 May 1968 at about 0315 UT (2015 midpath time) with the receiving array directed to an azimuth of 90 deg.

V. A NEW PROPAGATION MODE

The remarkable sensitivity and directivity of the 2.5 km Los Banos array as illustrated by Chapters III and IV have led to the discovery of a new mode of oblique ionospheric propagation which will be described here for the first time. This mode could not have been observed if the ionosphere did not support the 0.5 deg azimuthal resolution and the 8 μsec time delay resolution used for these tests. Consequently, the observability of this mode in itself demonstrates the excellent resolution obtainable over ionospheric paths. In addition to experimental observations of the mode, this chapter will present an explanation (with experimental verification) of the propagation mechanisms which produce the mode.

A. FIRST OBSERVATIONS OF A NEW MODE

Figure 18 shows two SFCW soundings made over the 2600 km path between Bearden and Los Banos with the full 256-element receiving array steered to 90 deg, the true transmitter bearing. Of particular interest are the discrete lines on the two-hop mode intermediate between the two-hop high ray (2F2H) and the two-hop low ray (2F2L). These were the first records in which such lines were observed so clearly that they implied a unique mode of propagation deserving further investigation.

B. EXPLANATION OF THE NEW MODE

The most likely explanation for this new mode can be described with the aid of Fig. 19. Here is shown (for a flat earth and flat ionosphere) the normal geometry for two-hop propagation at a single frequency. The low ray is represented by a solid line and the high ray is represented by a dotted line. If the midpath ground-reflection region is smooth, then for each ray the angle of reflection will equal the angle of incidence, and energy cannot transfer from one mode to the other during reflection. That is, for a smooth reflection region,

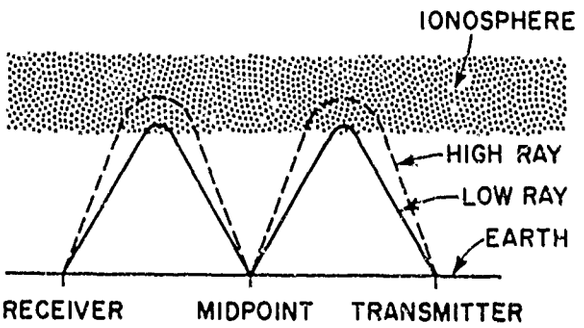

Figure 19 Simplified geometry for two-hop oblique ionospheric propagation at a single frequency.

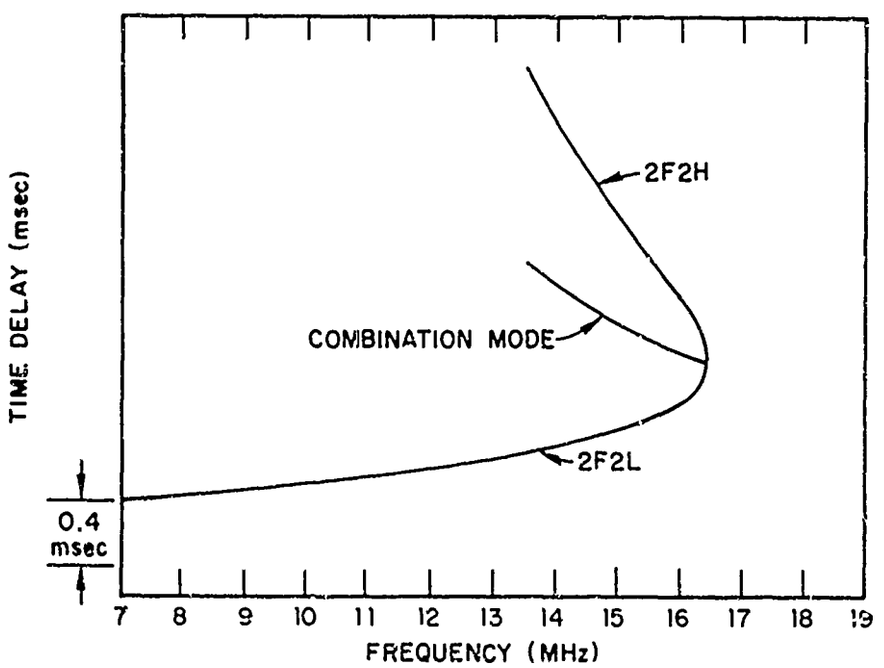

Figure 20 Two-hop ionogram generated by computer raytracing for a 2600 km path with equal length hops of 1300 km each.

energy that traveled the first hop via the low ray must also travel the second hop via the low ray; and energy that made the first hop via the high ray must make the second hop via the high ray.

If the midpath reflection region is rough rather than smooth, however, some energy may be transferred between modes by reflection. When this is the case, a two-hop mode may exist which makes one hop via low ray and the other hop via high ray. This "combination mode" has a time delay intermediate between two-hop high ray and two-hop low ray, and is believed to produce the additional discrete lines observed in Fig. 18.

Computer raytracing techniques developed by Croft [Ref. 23] were used to investigate the character of the combination mode for various ground reflection points at and away from the midpath point. The model ionosphere employed in these studies was a single Chapman layer with a vertical incidence critical frequency of 9 MHz and maximum ionization at an altitude of 300 km (ionosphere IID 165 in Ref. 23). The ionospheric profile was assumed constant over the path, and the effects of the earth's magnetic field were neglected.

Figure 20 shows a computer-generated two-hop ionogram for a 2600 km path with equal length hops of 1300 km each (1300/1300). It is assumed that energy may be transferred between high ray and low ray at the ground-reflection point, which gives rise to the combination mode shown in the figure. Notice the similarity between Fig. 20 and the two-hop portions of the experimental records of Fig. 18. The double lines of the new mode in Fig. 18 might be attributable to magnetoionic splitting produced by the earth's magnetic field, an effect neglected in the computer calculations for reasons of economy.

The midpath reflection for two-hop propagation over the 2600 km path between Bearden and Los Banos occurs in the Rocky Mountains, an unusually rough scattering region. These mountains provide the mechanism by which energy may be transferred between high ray and low ray at the midpath point. Since this roughness extends over a sizeable region, it is also possible for energy scattered by points some distance from the midpath point to propagate to the receiver. Consequently,

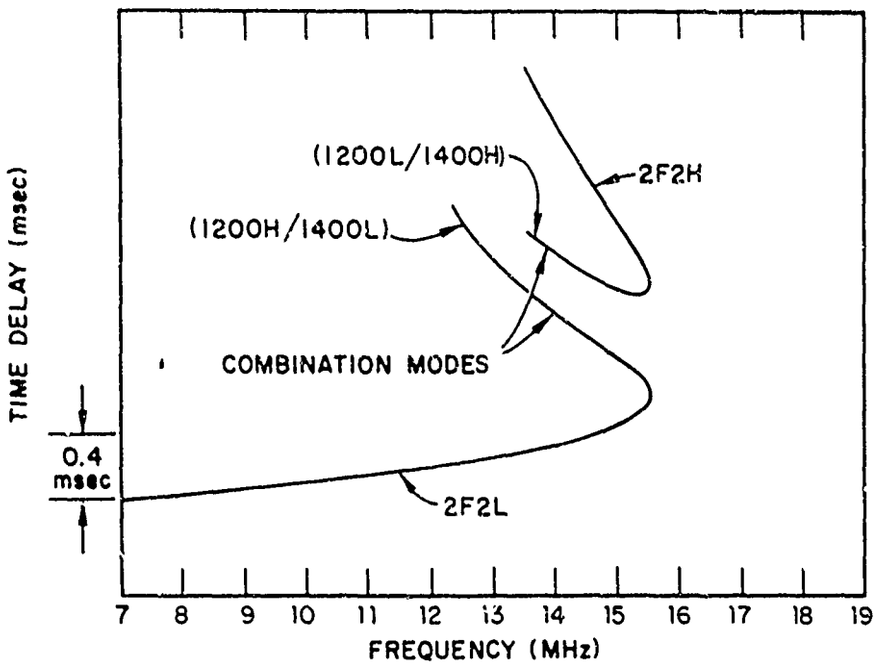

Figure 21 Computer-generated two-hop ionogram for a 2600 km path having one hop of 1200 km and the other hop of 1400 km.

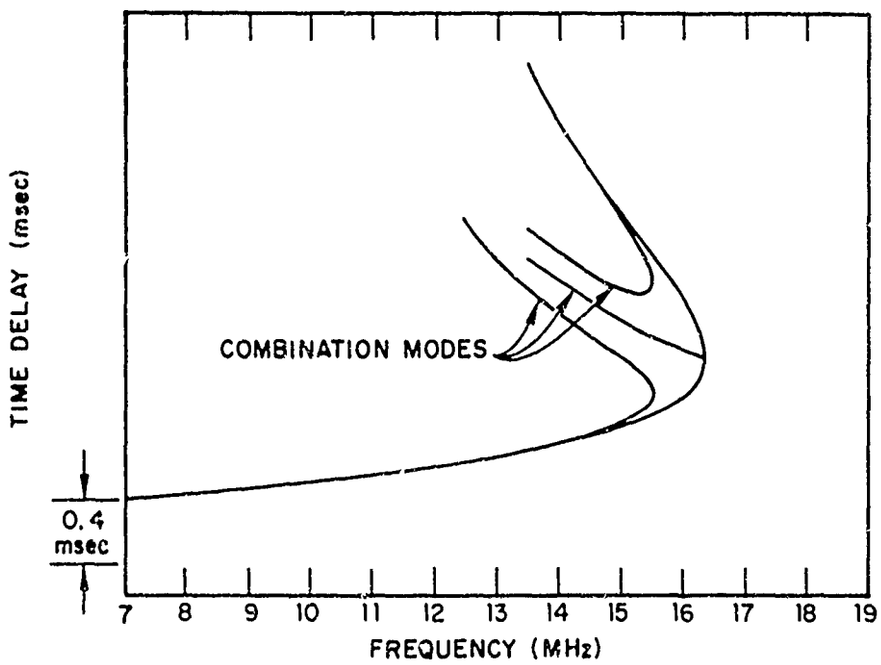

Figure 22 Superposition of two-hop ionograms from Figures 20 and 21.

reflection points for two-hop propagation from transmitter to receiver can occur closer to one station than to the other, so that one of the hops is actually longer than the other. In addition, reflections can occur off of the great circle path between stations, so that the total path is longer than the propagation path along the great circle.

Figure 21 illustrates the computer generated two-hop ionogram for a 2600 km path, where one hop is 1200 km and the other hop is 1400 km. In this case the combination mode consists of two components, one for which energy travels the 1400 km hop via high ray and the 1200 km hop via low ray (1200L/1400H), and the other for which energy travels the 1400 km hop via low ray and the 1200 km hop via high ray (1200H/1400L). The maximum observable frequency (MOF) for this two-hop mode is determined by the MOF of the 1200 km hop.

Since the actual ground reflection for the two-hop path between Bearden and Los Banos is produced by an ensemble of mountainous scatterers, the received signal will contain contributions from several different reflection points. To illustrate how this might appear, Fig. 22 shows the superposition of Figs. 20 and 21. In practice more than two scatterers are probably present; but Fig. 22 gives an indication of the general character to be expected.

C. ADDITIONAL OBSERVATIONS OF THE COMBINATION MODE

If the above explanation for the new mode is correct, then the combination-mode effect should occur over a range of azimuths around the true transmitter bearing. In addition, sensitivity to combination-mode energy should be increased by steering away from the true transmitter bearing to enable the receiving array directivity to discriminate against the strong, unscattered portion (specular component) of the received energy. This hypothesis is verified by the experimental records now to be described.

Figure 23 shows an SFCW sounding taken over the Bearden-to-Los Banos path with the receiving array directed to 92 deg (2 deg south of the true transmitter bearing). Notice the somewhat complicated

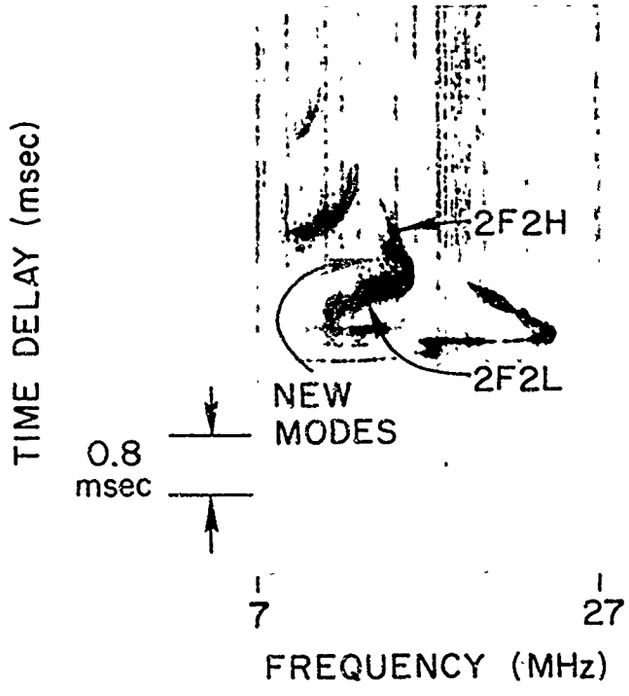

Figure 23 Ionogram taken 2 May 1969 at about 2200 UT (1500 midpath time). The receiving array was directed to an azimuth of 92 deg, 2 deg south of the true transmitter bearing.

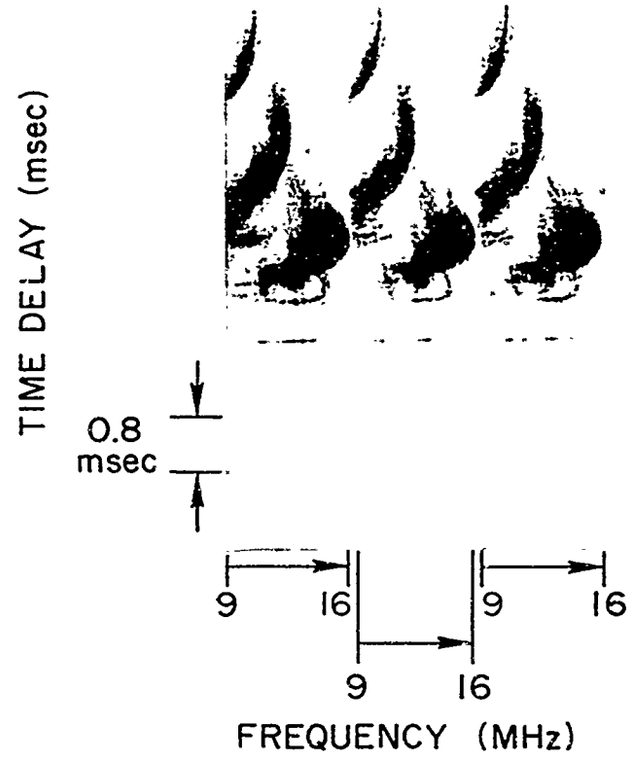

Figure 24 Soundings emphasizing the two-hop F2 propagation mode taken 30 sec apart on 2 May 1969 at about 2120 UT (1420 midpath time). The receiving array was again directed to an azimuth of 92 deg.

structure in the two-hop portion of the record between the high ray and the low ray. Such a structure is usually observed when operating in this manner, although its character varies somewhat with time and the array pointing direction.

In order to further emphasize the character of the mode structure just described, Fig. 24 shows additional records taken 30 sec apart with the array again directed to an azimuth of 92 deg. To optimize system sensitivity to the mode of interest, the frequency band swept was reduced for these records to include the two-hop F2 mode but to eliminate the one-hop F2 mode. Notice again the clearly apparent mode structure between the two-hop high ray and the two-hop low ray. This structure compares favorably in character with that in the computer-generated two-hop ionogram of Fig. 22. This result strongly supports the theory that the new mode structure is a result of the superposition of combination modes which are produced by ground scattering.

It should be emphasized that this mode structure could not be seen without high azimuthal resolution because so many scatterers (mountains) would lie within the beam that they would be indistinguishable. In addition, high time-delay resolution is necessary in order to resolve scatterers which lie within the narrow beam at different ranges. Time-delay resolution of 16 μsec or better was used for these tests.

D. VERIFICATION OF THE "COMBINATION-MODE" EXPLANATION

Although it was felt that the mechanism producing the new mode described in the preceding section was transfer of energy between low and high rays by rough scatterers at the ground reflection point, the possibility still remained that the mode might be attributable to other forms of complex propagation such as different ionization profiles at the two ionospheric reflection points, or interlayer propagation within the ionosphere. To verify further the combination-mode theory, a portable repeater [Ref. 24] was operated at a location in north-central New Mexico very near the midpath reflection point for the Bearden-Los Banos path. The repeater served as a large discrete

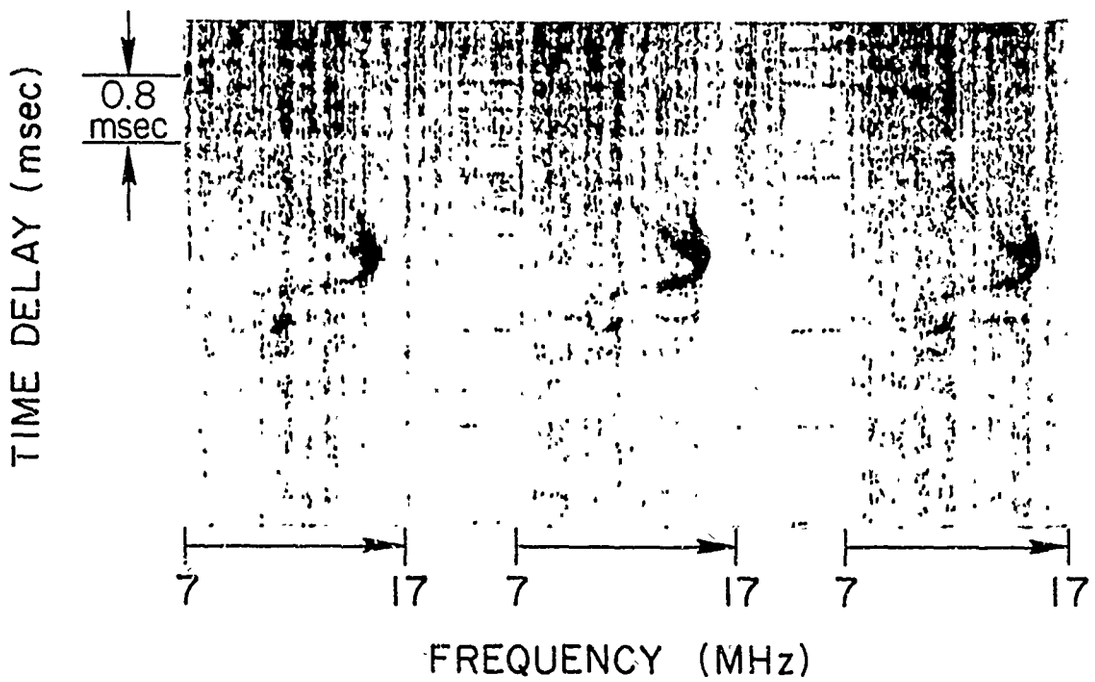

Figure 25 Soundings showing echoes from a repeater operating near the midpath point of the Bearden-to-Los Banos path.

These records were taken on 16 May 1969 at about 2350 UT (1650 midpath time).

scatterer which received signals from almost any vertical angle and retransmitted them over a wide continuum of vertical angles. In addition, the repeater shifted the frequency of the received signals slightly before retransmitting them, allowing separation of the repeated energy from the ground reflected energy at Los Banos. Hence the repeated modes received at Los Banos were guaranteed to have come down at the midpath point, and efficient transfer of energy between high and low rays during reflection was assured.

Operation of the portable repeater near the midpath point on 16 May 1969 verified the existence of the combination mode on two-hop oblique propagation. Examples of two-hop records which display only the repeated energy are shown in Fig. 25. The combination mode can be clearly seen. As expected, this figure compares well with Figs. 18 and 20.

VI. DIGITAL FORMATION OF MULTIPLE BEAMS

Chapter I described an investigation which measured received signal amplitude and phase distributions across the 2.5 km array. Because of equipmental limitations, that experiment was restricted primarily to CW operation at frequencies propagating only a single mode in order to eliminate multimode interference. In practice, such restrictions permitted only daytime study of one-hop F2 low ray for frequencies at about 0.7 of the MOF, a very severe limitation.

Chapter III described another technique which measured the azimuthal distributions of received signals on a mode-resolved basis, with the advantage that it can be used to study, individually, all modes at any frequency at any time of the day or night. In addition, data processing is inexpensive and is done in real time. The technique also has a few drawbacks. A once-per-second frequency sweep over a 250 kHz bandwidth sometimes produces objectionable interference to other users of the HF spectrum. Each azimuth scan requires nearly a minute to accomplish, and it is not always safe to assume that the ionosphere varies slowly compared to the time span of a minute. Finally, the facsimile recorder, like other types of intensity-modulated displays, provides only a qualitative measure of amplitude and has a severely restricted dynamic range.

This chapter will describe a new experimental technique developed by the author which permits both azimuthal analysis and measurement of array amplitude and phase distributions for mode-resolved signals on a quantitative basis and with a much higher dynamic range. The interference to other HF users is greatly reduced by using this technique; and the length of time needed to acquire data for a single record is short compared to the time involved in ionospheric changes.

The technique incorporates extensive digital processing which, in itself, is a new development in HF array signal combining and processing.

Preceding page blank

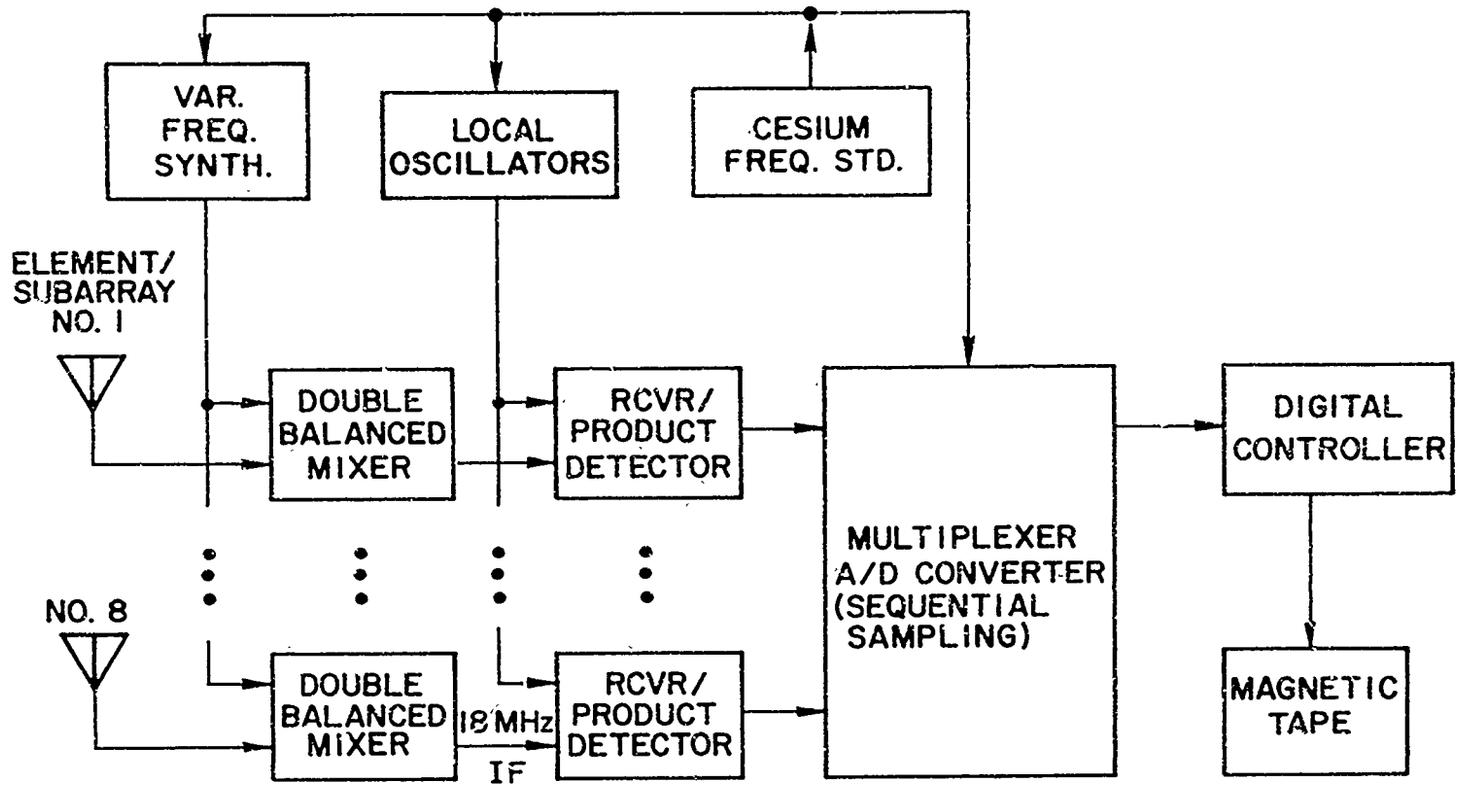

Figure 26 Block diagram of the eight-channel receiving and digital recording system for the Los Banos array.

A. EXPERIMENTAL ARRANGEMENT

The experimental technique to be described uses eight subarrays of the Los Banos receiving array. The subarrays are uniformly spaced apart by 320 meters along a north-south line, providing an aperture more than 2.5 km in length. The SFCW signals used for this experiment were transmitted from Bearden, Arkansas, which as already noted is 2600 km east of the receiving site with a bearing perpendicular to the line of the array. As before, mode structures were identified on the basis of sweep-frequency oblique soundings over the path.

The receiving and recording system, which consists of eight identical channels to coherently process the eight subarray outputs, is illustrated by the block diagram of Fig. 26. All feed lines are precisely matched in length to the inputs of this system as described in the Appendix. The first stage in each channel is a broadband conversion made with a variable frequency synthesizer serving to deramp incoming SFCW signals. The desired input signals are translated by this stage to 18 MHz intermediate frequencies, where they are filtered and converted to audio frequencies by coherent, product-detector receivers fix-tuned to 18 MHz. The product-detector outputs of the eight channels are sequentially sampled, converted to digital form and stored on magnetic tape for later processing. For these tests each receiver had a 2 kHz bandwidth. All of the injection frequencies used in the system, including the variable frequency synthesizer, the receiver local oscillators, and the sampling frequency are derived from a single cesium frequency standard, thereby providing extremely high frequency stability and accuracy, and complete system coherence.

The eight channels are matched in amplitude and phase by calibration so that the amplitude and phase distribution at the system output is the same as the amplitude and phase distribution at its input. For calibration purposes the elements at the inputs of the system may be replaced by eight isolated signals of equal amplitude and phase by simply flipping a switch. This is done frequently during the course of operation to insure proper system calibration.

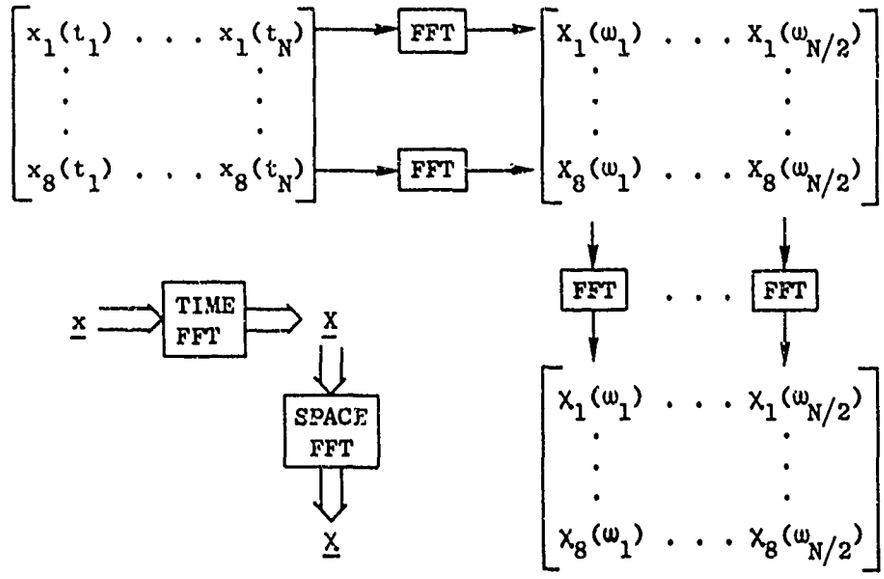

Figure 27 Basic digital data-processing scheme for determining signal spectrum vs azimuth.

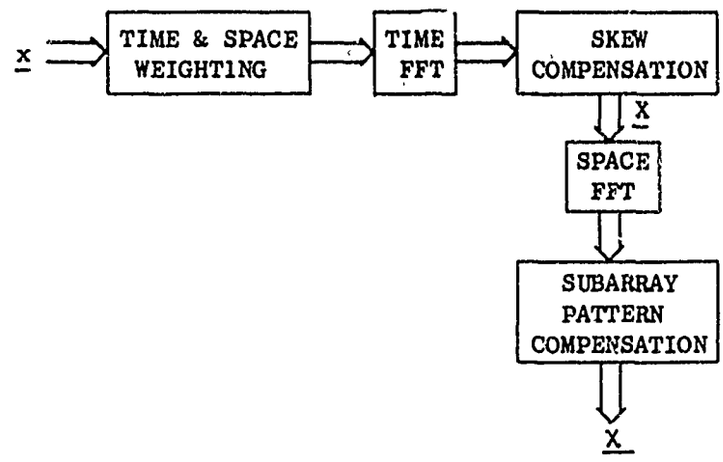

Figure 28 Block diagram of the complete digital processing scheme, showing modifications to the basic scheme of Figure 27.

B. DATA PROCESSING

Digital magnetic tapes recorded with the system of Fig. 26 contain sampled versions of the voltage outputs of the product detectors for each of the eight receivers. Sampling is sufficiently fast to prevent spectral aliasing, and enough samples are taken to provide the desired frequency resolution.

These digital tapes are processed on an XDS Sigma 5 computer to provide spectrum analyses of received signals for eight different azimuths simultaneously. The processing to accomplish this is illustrated by Fig. 27. Here the $\underline{x}$ matrix represents the time samples recorded on the magnetic tape. The matrix element $x_i(t_j)$, a real-valued number, represents the voltage output of the ith receiver (i^{th} antenna) at the jth sampling time. Calculating the Discrete Fourier Transform (DFT) for each row of the matrix by using the Fast Fourier Transform (FFT) computer algorithm [Ref. 25], provides a spectral analysis of each receiver output. Since there are N real-valued samples in each row, each FFT will produce $\frac{N}{2}$ unique complex-valued numbers which are illustrated in Fig. 27 as a new matrix $\underline{X}$. In this matrix the element $X_i(\omega_j)$ represents the amplitude and phase of the ith receiver at the jth frequency sample (frequency cell). The rows of this matrix represent the spectral output of each receiver, while the columns represent the amplitude and phase distribution across the array for each spectral component.

Since the array pattern is related to the Fourier Transform of the amplitude and phase distribution across the array [Ref. 26], performing an FFT on each column of the $\underline{X}$ matrix produces eight unique samples of the array pattern for each spectral component. The result of transforming the columns of the $\underline{X}$ matrix is illustrated as matrix $\underline{\chi}$ in Fig. 27. The element $\chi_i(\omega_j)$ represents the amplitude and phase of the jth spectral component at the ith azimuth. In other words, this matrix contains the received signal spectrum versus azimuth, and is equivalent to spectral analyses of eight simultaneous beams.

The processing illustrated by Fig. 27 will be recognized as a two-dimensional Fourier transform. Its calculation is complicated

somewhat by the fact that the eight channels in the recording system are sampled sequentially rather than simultaneously in time. To correct for this a "skew compensation" is applied to the $\underline{X}$ matrix which consists of a different linear-phase versus frequency correction made for each row. In addition, to provide low spectral and azimuthal sidelobes, a "Hanning" window is used for time weighting [Ref. 27] and a "Dolph" taper is used for space weighting [Ref. 18]. Finally, since the subarrays attenuate the beams synthesized away from boresite with respect to the boresite beam, a subarray pattern compensation is applied to matrix $\underline{X}$. The complete processing is illustrated by the block diagram of Fig. 28.

As explained in Chapter II, spectrum analysis of a deramped SFCW signal enables measurement of time delay. Consequently, when processing deramped SFCW signals, matrix $\underline{X}$ of Fig. 27 contains amplitude and phase versus time delay for each of the eight subarrays. Furthermore, matrix $\underline{X}$ contains amplitude and phase versus time delay for each of eight azimuths.

If the period between samples for each channel (receiver outputs of Fig. 26) is T sec and there are N samples per channel, then the frequency resolution obtained is about $\frac{1}{NT}$ Hz. For a sweep rate of s Hz/sec, this provides a time delay resolution of about $\frac{1}{NTs}$ sec. Similarly for eight subarrays whose centers are spaced by 320 m, and a received signal wavelength of λ, the spacing between beams is

$$\frac{1}{(8)(320/\lambda)} = \frac{\lambda}{2560} \text{ radians} .$$

All of the data necessary to synthesize eight beams are recorded simultaneously, so that it is necessary to sweep through any single frequency only once to produce a complete display. Typically, a sounding through the HF spectrum requires two minutes to complete. Consequently, the transmitted signal will pass through a single frequency only at intervals of two minutes or greater, producing a click very similar to those ordinarily heard at HF from other sources. As a result this sounding produces very little interference to other HF users.

C. EXAMPLES OF EXPERIMENTAL RESULTS

Digitally produced displays of amplitude versus group delay and azimuth for a single ionogram will be presented in this section. The data were recorded using a sweep rate of 250 kHz/sec and a sampling rate of 16 kHz (2 kHz per channel).

To illustrate the mode structure existing at the time, Fig. 29 shows the digitally processed ionogram generated with the data from channel one of the digital recording system. This figure is actually composed of 96 individual displays of received signal amplitude (horizontal displacement) versus time delay (vertical displacement) at a particular transmitted frequency. Each display consists of the amplitudes of the 512 points produced by a 1024 real-point FFT. The 96 displays are linearly spaced along a horizontal frequency scale to produce the ionogram of Fig. 29.

Displays of received signal amplitude versus time delay and azimuth for selected frequencies are shown in Fig. 30. The display for each frequency was produced with the processing shown in Fig. 28 where the matrix $\underline{x}$ contained 8192 real points (1024 points for each channel). Since the sampling rate was 16 kHz, only about 0.5 sec of data is required to produce a display, a time interval short compared to ionospheric fluctuations. The sweep-rate of 250 kHz/sec provided a time delay resolution of about 8 μsec. The processed matrix, $\underline{X}$, contains 4096 complex points (512 points per beam), and it is the amplitudes of these points which are displayed in Fig. 30.

The display for each frequency is actually composed of nine plots, one for each beam or azimuth, where amplitude is shown as increasing linearly to the right and time delay as increasing vertically upward. Each display is normalized so that its largest amplitude has a standard displacement. The plots for the separate beams are spaced apart by this normalized displacement and arranged in order, with azimuth increasing to the right.

The leftmost and rightmost plots of each display are identical as a consequence of spatial aliasing. That is, if the main beam of the array were steered within the subarray pattern to the position of the

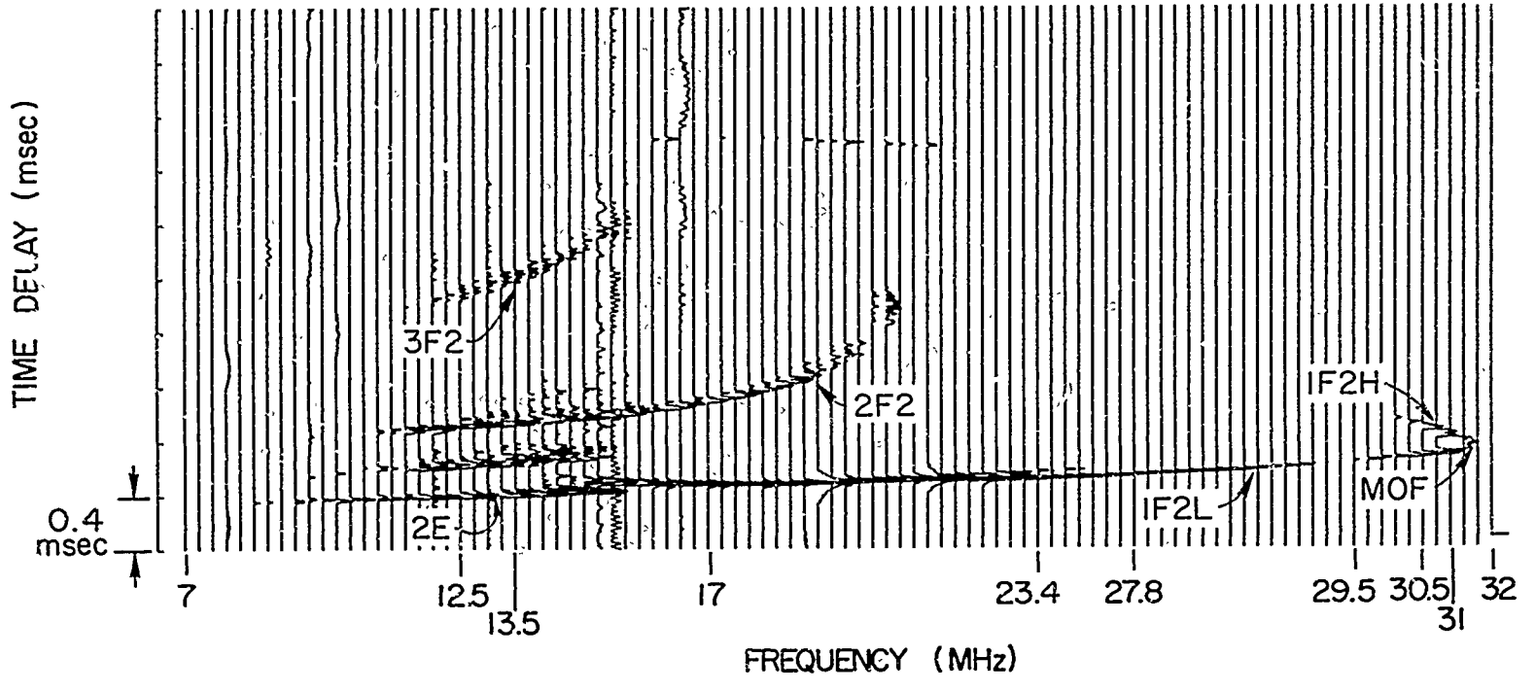

Figure 29 Digitally processed ionogram for a sounding received with a single Los Banos subarray on 28 Mar 1969 at 2236 UT (1536 midpath time).

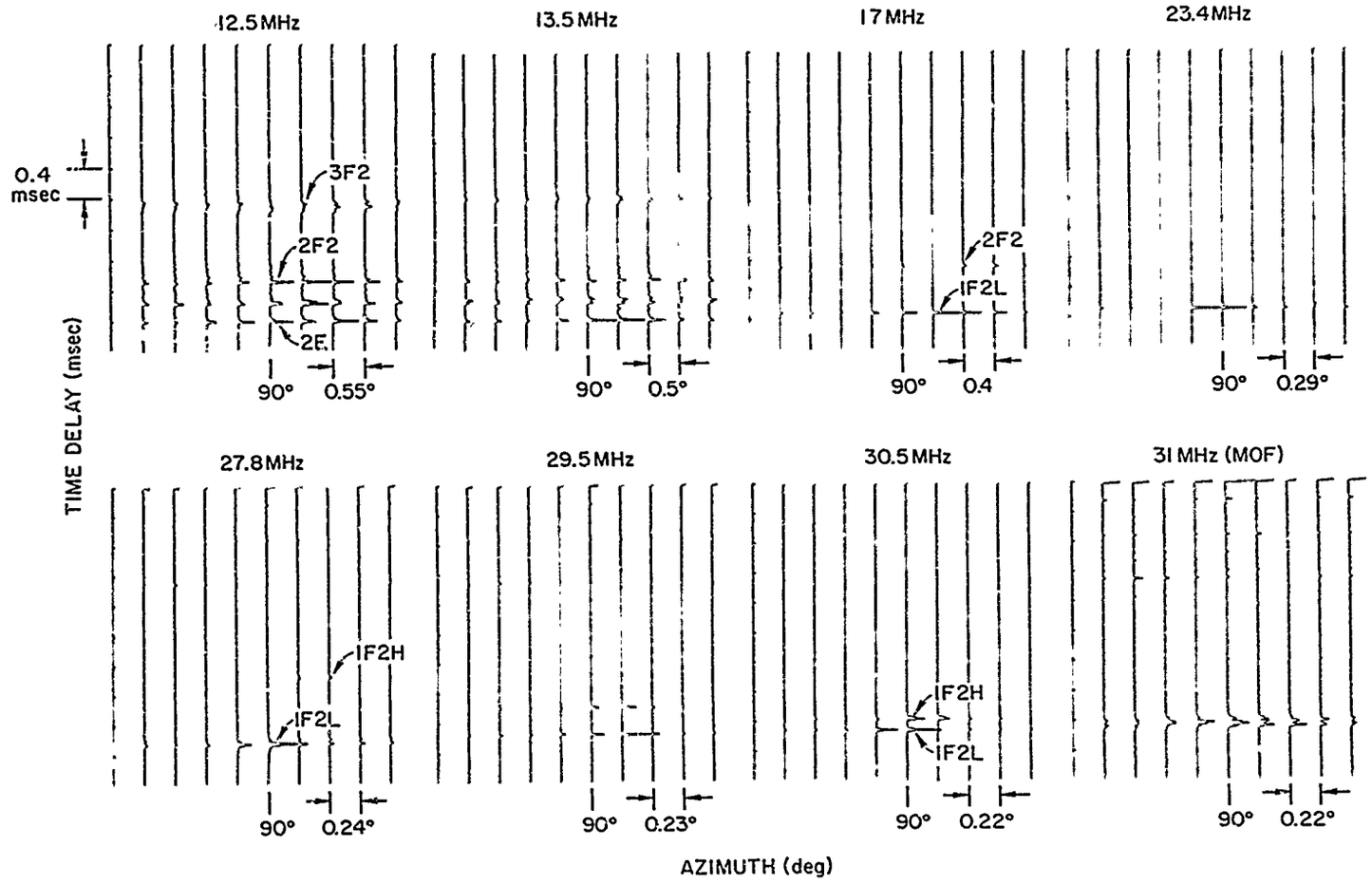

Figure 30 Digitally processed displays of received signal amplitude vs time delay at 9 azimuths for various frequencies selected from the ionogram of Figure 29.

rightmost beam, the first grating lobe would appear at the position of the leftmost beam. The subarray pattern itself helps to eliminate other ambiguities by attenuating energy arriving from wider angles.

The various signal components appearing on Fig. 30 can be identified by the aid of Fig. 29. For example, at 30.5 MHz, reflections due to 2 modes are visible: 1F2L and 1F2H. It should be noted that in Fig. 30 the 1F2H mode is clearly visible at 27.8 MHz, whereas such is not the case in Fig. 29. This is because the full array was used for Fig. 30, whereas only one subarray was used in Fig. 29. The full array provides an effective 9 dB of gain with respect to a subarray.

There are two particularly interesting features of Fig. 30. The first is that the one-hop F2 low ray is discrete in azimuth except at 17 MHz where it appears spread over 1.5 deg. This spread is quite unusual and is possibly due to a polarization null being present in the 125 kHz of data used to produce this display. The other interesting feature is the spread in azimuth of the energy observed at the 31 MHz maximum observable frequency (MOF). Although this appears to be a common occurrence, no satisfactory explanation for it has yet been found.

Displays such as those in Fig. 30 allow quantitative study of the influence of ionospheric propagation upon the spatial properties of HF signals. In general, however, these lead to the same conclusions as reached in Chapter IV. Modes without ground reflections appear discrete in azimuth and time delay, while modes with ground reflection appear spread in azimuth and time delay. The one-hop F2 low ray is usually within 0.25 deg of the true transmitter bearing, and the high ray usually arrives south of the low ray.

As mentioned earlier, the amplitude and phase distribution for any mode can also be found using this digital processing technique. This is done by displaying the amplitude and phase of the eight subarrays relative to subarray number one as found by selecting the appropriate column (time delay) from the matrix $\underline{X}$ of Fig. 27.

Two results of this procedure are shown in Fig. 31. The lower part of this figure presents two displays, similar in nature to those of

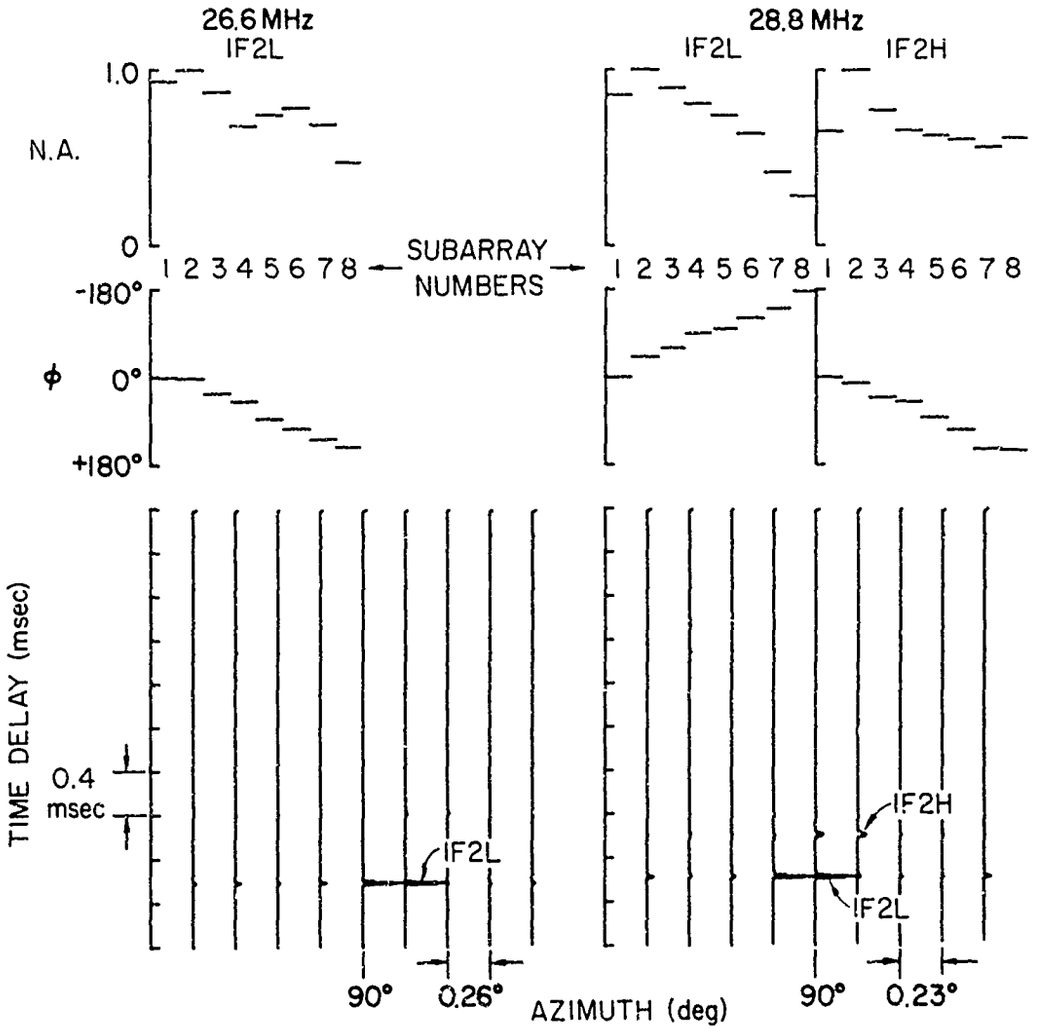

Figure 31 Digitally processed displays of received signal amplitude vs time delay at 9 azimuths (bottom) and distributions of amplitude and phase across the receiving array (top) for selected modes from the ionogram of Figure 29.

N.A. = Normalized amplitude.
φ = Phase relative to subarray No. 1.

Fig. 30, for frequencies of 26.6 MHz and 28.8 MHz, respectively. These displays correspond to the amplitudes of the matrix $\underline{X}$ in Fig. 27. The computer automatically selected the strongest mode or modes for the amplitude and phase displays shown at the top of this figure. The values for these latter displays are taken from matrix $\underline{X}$ in Fig. 27 and represent each of the 8 different subarrays. Notice the reasonably linear phase distributions which give rise to the discrete azimuths of the modes.

These examples illustrate the usefulness of this new experimental technique. The ability to measure the azimuthal distributions of modes as well as their amplitude and phase distributions quickly and conveniently, with a minimum of interference to others provides a powerful means of ionospheric investigation which is only just beginning.

VII. DIGITAL MEASUREMENT OF IONOSPHERIC DOPPLER VERSUS AZIMUTH

The experimental technique described in the previous chapter can also be used, with only slight modification, to measure ionospheric doppler spectra versus azimuth. The present chapter will show that ionospheric modes, at least at times, can be resolved on the basis of their different doppler characteristics and, once resolved, may be identified on the basis of their azimuthal properties. This capability has never before been demonstrated, and establishes the feasibility of mode-resolved azimuthal studies using CW at any arbitrary radio frequency.

A. EXPERIMENTAL ARRANGEMENT

The sites and equipment used in this experiment are identical to those described in Chapter VI with the following exceptions:

1. Data were taken with CW transmissions instead of SFCW transmissions. (SFCW was used only for occasional soundings over the path to assist in identifying propagation modes.)
2. In the digital recording system of Fig. 26 the variable frequency synthesizer, rather than sweeping in frequency, was fixed tuned to select the CW frequency of interest.
3. Eight elements of the array (vertical whips) uniformly spaced by 360 meters were used instead of subarrays at the system input.
4. Receiver bandwidths of 200 Hz were used in place of the 2 kHz bandwidths used before.

B. DATA PROCESSING

Data processing in this experiment was identical to that described in Chapter VI except that, since vertical whips were used instead of subarrays, the subarray pattern compensation was eliminated. In addition, since the received signal was CW, the matrix $\underline{X}$ of Fig. 27 produced the doppler spectrum versus azimuth instead of time delay versus azimuth.

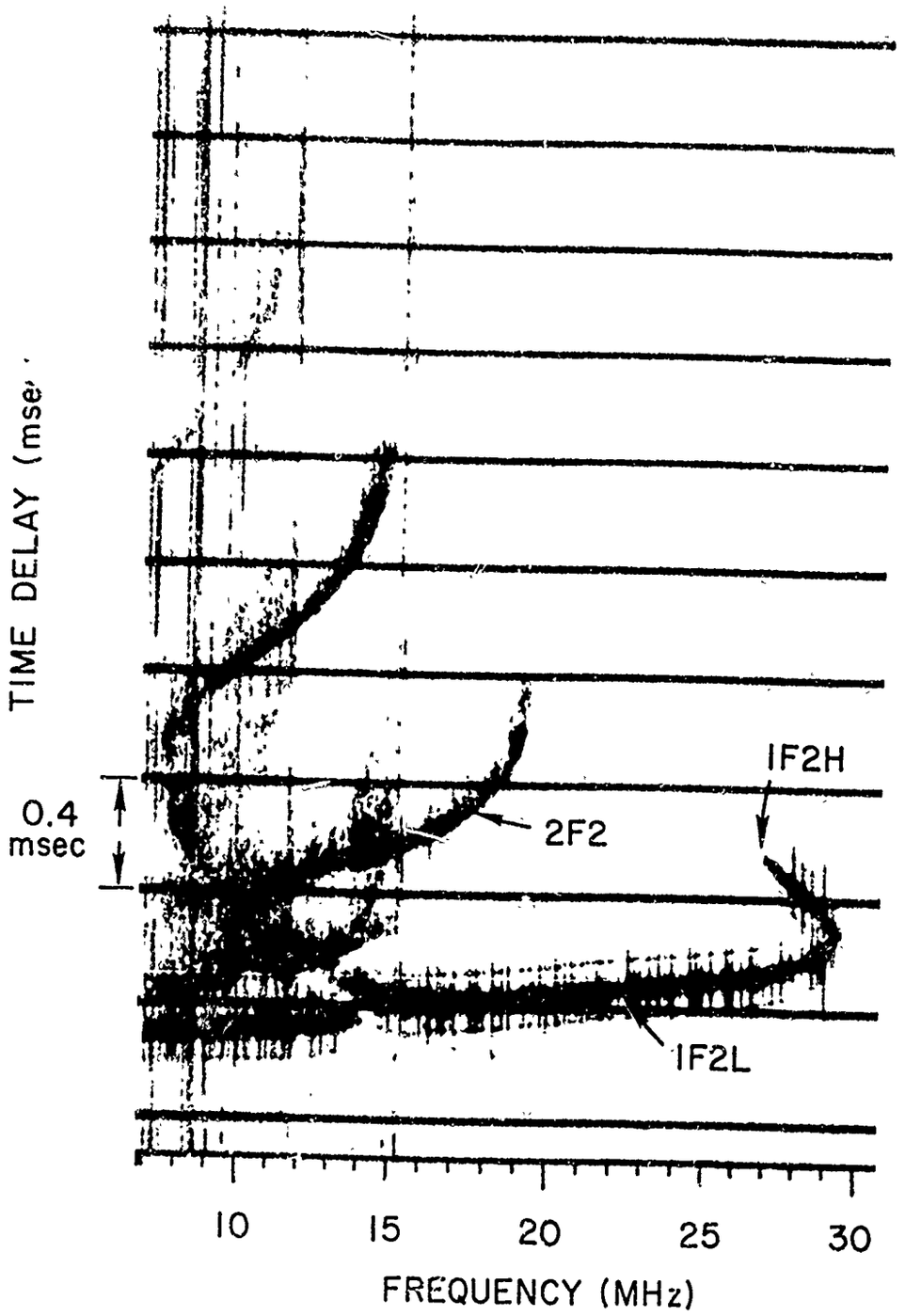

Figure 32 Ionogram taken 15 Jan 1970 at about 2130 UT (1430 midpath time).

In recording these data, a sampling rate of 500 samples per second was used, providing a sampling rate for each channel of 62.5 samples per second. Since ionospheric doppler is usually confined to about a 2 Hz bandwidth, sampling was far faster than necessary and many more samples were recorded than necessary. This was done as an expedient in order to utilize the existing processing program, although as a consequence, data processing required far more computer time than was really necessary. A total of 4096 samples (512 samples per channel) were processed at a time representing 8 seconds of data and providing a doppler resolution of about 1/8 Hz. The azimuthal resolution was a function of frequency but typically was 1/4 deg.

C. EXPERIMENTAL RESULTS

Examples of experimental records showing ionospheric doppler versus azimuth will be presented in this section.

Figure 32 shows an oblique sounding taken prior to the doppler-azimuth records to be shown and illustrating the ionospheric mode structure existing over the path at the time.

Figure 33 shows the processed doppler-azimuth output for a calibrate signal applied to the system. The calibrate signal represents a source of zero doppler shift on the array boresite. The upper display of the figure shows the system output frequency versus azimuth, and is the same as the displays in Chapter VI except that the signal amplitude in an individual doppler cell is represented by a dot and the dots are not interconnected as they were before. Adjacent dots are 1/8 Hz apart. In addition, the largest doppler component on the display is normalized to have a displacement of 0.8 the spacing between adjacent beams. Notice that the system injections were set to place zero doppler at a system output frequency of 15 Hz, and that the array boresite has a bearing of 90 deg true.

The length of the shorter vertical line on the far right of the display represents (logarithmically) the amplitude of the largest doppler component and provides a measure of the normalization factor used in producing the display.

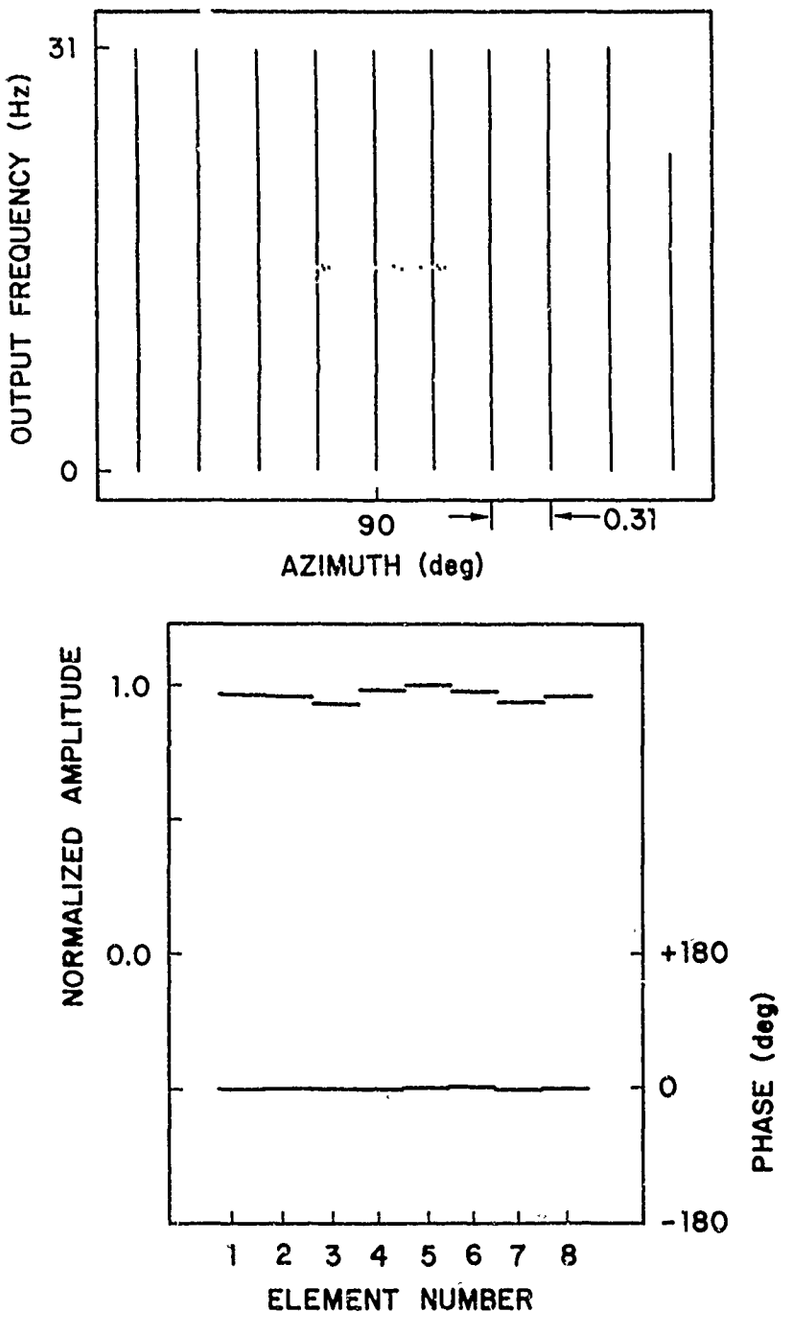

Figure 33 Digitally processed displays of received signal amplitude vs frequency at 9 azimuths (top) and distributions of amplitude and phase across the array for the strongest frequency component (bottom) with a calibration signal applied to the input of the receiving system.

The lower display in the figure represents the distributions of amplitude and phase across the array for the strongest doppler component of the upper display. Phases are measured with respect to the first element. The variations in amplitude illustrate the inaccuracies ordinarily present in calibrating the system. (The computer can, of course, compensate for such calibration errors, although this was not being done at the time these records were made.)

The display of doppler versus azimuth for a CW signal from Bearden at a frequency propagating only one-hop F2 low ray (1F2L) is shown in Fig. 34 along with the display of the distributions of amplitude and phase for the strongest received doppler component. Notice that the 1F2L mode is well-defined both in doppler and in azimuth (discrete to within the system resolution) and that the apparent transmitter bearing for this mode is only 0.1 deg north of the actual transmitter bearing of 90 deg true. This is completely consistent with the observations of azimuthal distributions of 1F2L when observed with modes resolved in time delay as discussed in Chapters IV and VI. Azimuthal sidelobes are down by roughly 20 dB. Notice that although the amplitude distribution across the array of the strongest doppler component fluctuates by ± 2 dB the phase distribution is quite linear.

The same displays for a frequency propagating both one-hop F2 (1F2) and two-hop F2 (2F2) are shown in Fig. 35. Here a large component appearing discrete both in azimuth and doppler is seen at a bearing of 90 deg. This component is probably the 1F2 mode which is known to show little spreading in azimuth. The other energy which appears spread both in azimuth and in doppler is associated with the 2F2 mode which has been shown in general to be spread in azimuth. The dispersed doppler was somewhat unexpected. This evidence shows that the ground reflected mode not only has a different doppler shift, but a different doppler character. It is apparently spread in group delay, in azimuth and in doppler.

Notice that the narrow beamwidth of this eight-element array is able to reject some of the 2F2 energy while not rejecting 1F2 energy, thereby increasing the ratio of one-hop to two-hop energy. This could

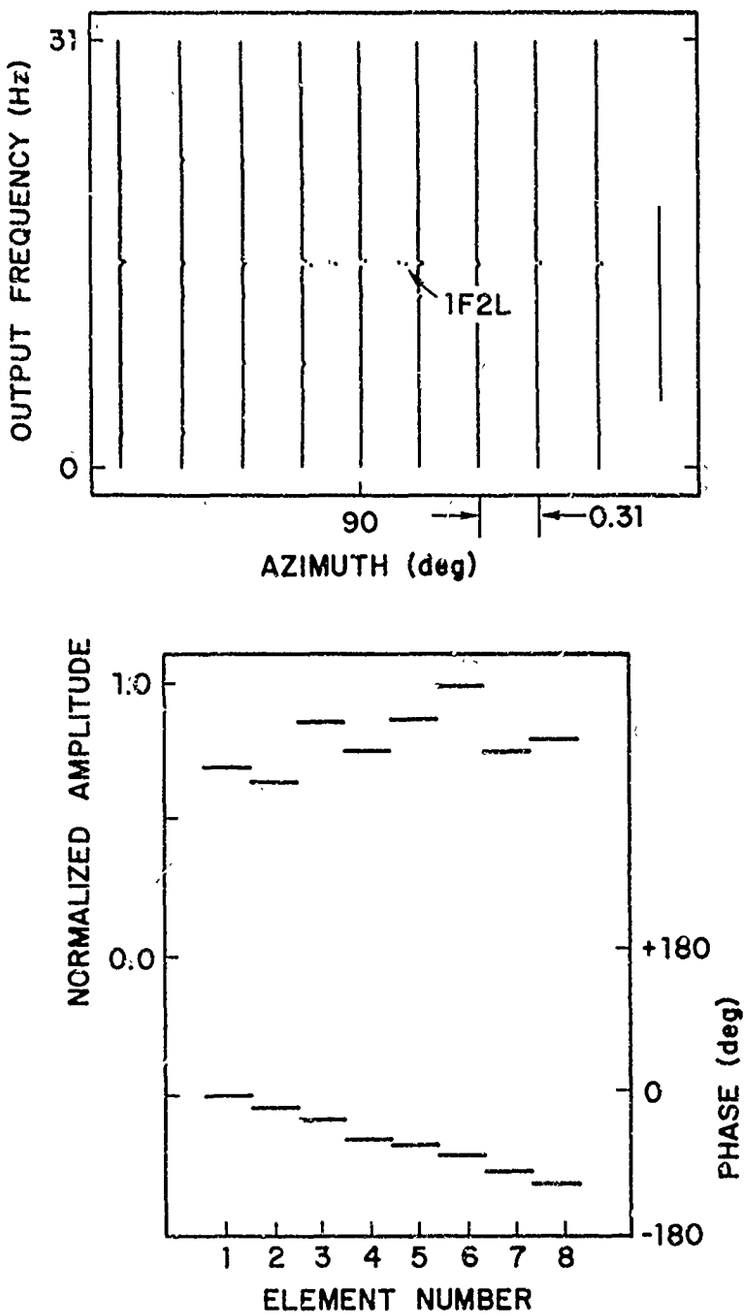

Figure 34 Digitally processed displays for a CW signal received at a frequency for which only one-hop F2 low ray (1F2L) was propagating.

The data shown were taken at 21.550 MHz on 15 Jan 1970 at about 2235 UT (1535 midpath time).

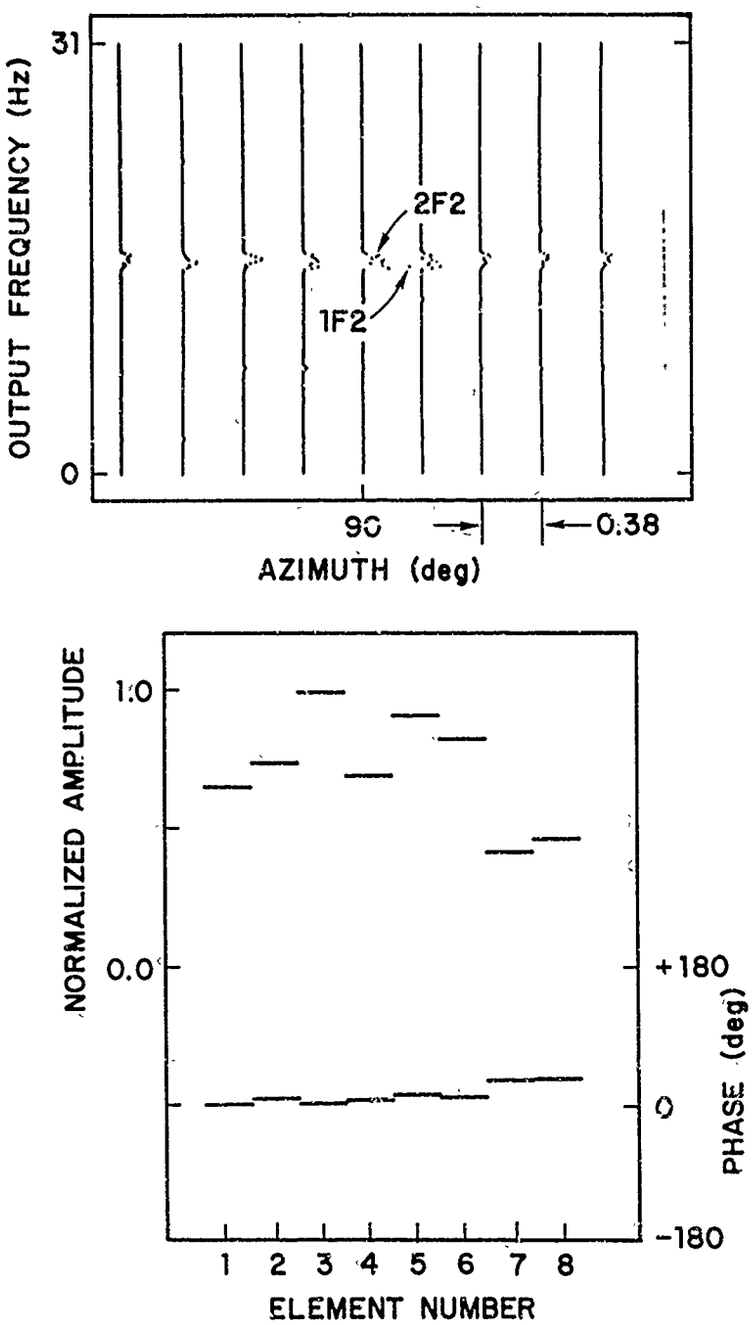

Figure 35 Digitally processed displays for a CW signal received at a frequency for which both one-hop F2 low ray (1F2L) and two-hop F2 (2F2) were propagating.

The data shown were taken at 17.833 MHz on 15 Jan 1970 at about 2310 UT (1610 midpath time).

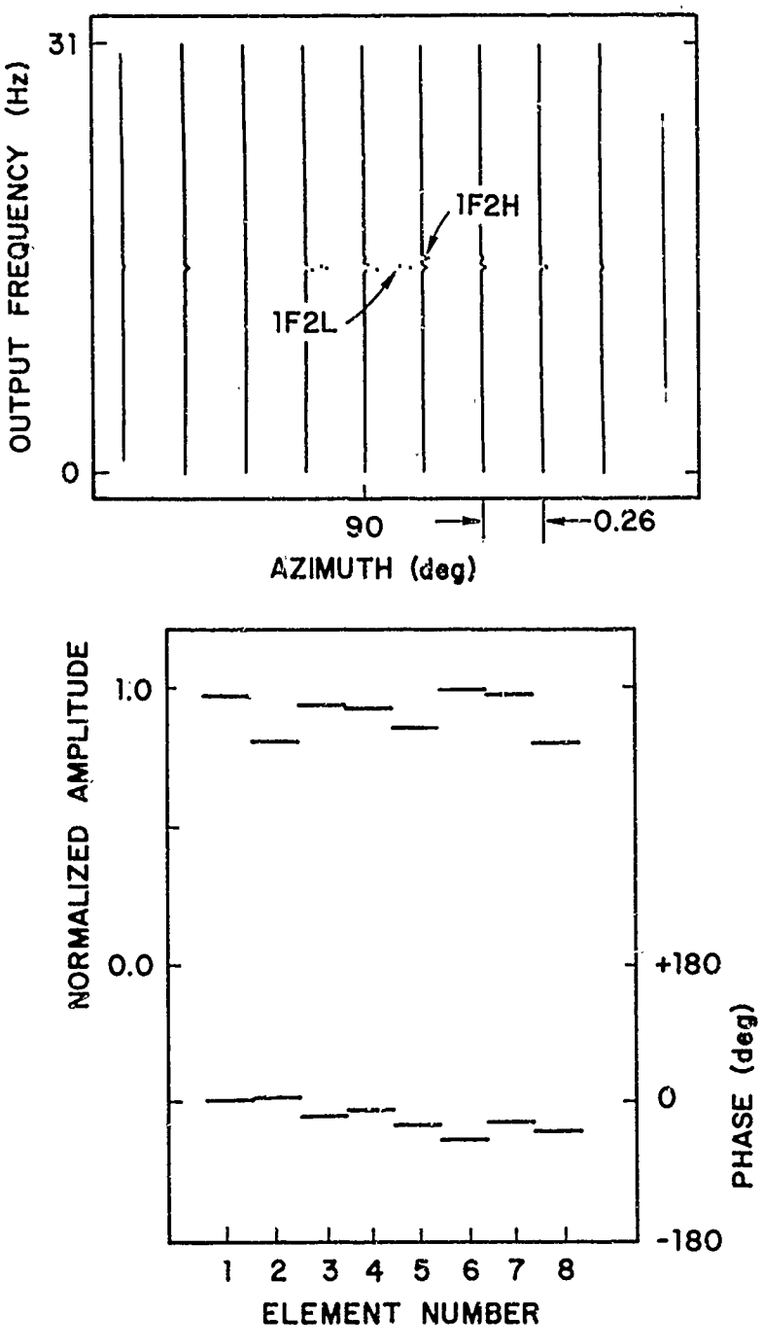

Figure 36 Digitally processed displays for a CW signal received at a frequency for which both one-hop F2 low ray and high ray (1F2L and 1F2H, respectively) were propagating.

The data shown were taken at 26.075 MHz on 15 Jan 1970 at about 2315 UT (1615 midpath time).

reduce the magnitude of fades produced by interference between these two modes if the beam could be kept pointing in the direction of arrival of the one-hop mode. In addition, since the one-hop F2 low ray ordinarily has an angle of arrival very close to the true transmitter bearing, the ability to distinguish between 1F2 and 2F2 on the basis of their doppler and azimuthal characteristics should allow much more accurate estimation of the transmitter bearing.

Figure 36 shows displays for a frequency which was propagating both one-hop F2 high ray and low ray (1F2H and 1F2L, respectively). Two components having distinct azimuths and dopplers are present. The smaller of these components is deviated about 1/4 deg south of the true transmitter bearing and is identified as the high ray (1F2H), since the high ray is known to often be deviated to the south and is usually smaller in amplitude than the low ray due to defocusing. The larger component associated with the low ray (1F2L) is deviated less than 0.1 deg north of the true transmitter bearing. Natural ionospheric doppler enabled separation of the two modes and knowledge of their azimuthal and amplitude characteristics enabled their identification. The display of amplitude and phase distributions across the array is for the 1F2L mode.

Additional data of the kinds shown above for different daytime hours and on other days have revealed that modes can often be resolved in doppler and identified in azimuth during the day, although not always. The fact that they can be resolved and identified by doppler-azimuth processing is a new result, as is the observation that the 2F2 mode exhibits a spread in doppler. This doppler spread is probably a consequence of scattering produced by the Rocky Mountains at the midpath ground reflection region.

VIII. CONCLUSION

A. SUMMARY OF RESULTS

In order to determine the influence of oblique ionospheric radio propagation upon the performance realized by a very large HF array, a 256-element, 2.5 km broadside array has been constructed, and used to receive signals propagated over a 2600 km east-west path. To simplify implementation of this array a new technique invented by the author for matching the lengths of very long feedlines was shown to provide outstanding precision and convenience. Through the use of SFCW soundings, propagation modes were identified and their azimuthal properties were individually studied with the 2.5 km array.

It was found that the sensitivity conferred by the combination of SFCW sounding and the very directive receiving array permitted useful ionospheric research to be conducted with transmitted powers as low as 5 mW. Use of such low powers virtually eliminates interference to other users of the HF spectrum. In addition, broadband signals transmitted with peak powers as remarkably low as 50 μW were received over the 2600 km path used for this study.

Daytime studies of individual modes conducted with the 2.5 km array revealed that single-hop modes usually appear discrete in azimuth and time delay to within the resolution of the system, while ground-reflected modes are generally spread both in azimuth and time delay. During quiet conditions, the one-hop F2 low ray was observed to have an angle of arrival usually within 0.25 deg and always within 0.5 deg of the true transmitter bearing. The one-hop F2 high ray was found to commonly arrive south of the low ray. This tendency was hypothesized to be a consequence of ionospheric tilts having north-south slopes which increase with altitude. The plausibility of this explanation was confirmed by three-dimensional computer raytracing with a model ionosphere based upon vertical ionosonde data.

A new propagation mode was discovered which is thought to result

Preceding page blank

from two-hop propagation in which one hop travels via high ray and the other via low ray. This new mode has been called a "combination mode". The existence of such a mode requires rough scattering at the midpath reflection region to enable transfer of energy between high and low rays. Such scattering is present for the path used in this study as a consequence of the fact that the midpath point lies in the Rocky Mountains. This explanation for the combination mode was substantiated analytically by computer raytracing, and experimentally by operating an HF repeater at the path midpoint.

A new experimental technique was developed and tested which measures amplitude versus time delay at eight azimuths simultaneously, with each azimuth having the resolution of the full 2.5 km array. The data for all eight azimuths are recorded within a time interval which is very short compared to the intervals of ionospheric changes. The use of SFCW transmissions provides average transmitted powers equal to peak powers, and excellent interference immunity. Interference to other stations is greatly reduced compared to previous methods because only a single frequency sweep is required to record all eight azimuths. The new technique makes extensive use of digital processing, and allows greatly improved flexibility, accuracy and dynamic range compared to previous techniques. In addition, the technique allows the distributions across the array of received signal amplitude and phase to be measured individually for any and all propagation modes--a useful and powerful capability.

Finally, measurement of ionospherically induced doppler shifts versus azimuth for obliquely propagated CW signals demonstrated that, when modes could be resolved in frequency on the basis of their different doppler shifts, they could often be identified on the basis of their azimuthal properties. This was accomplished by receiving with only eight whips spaced uniformly across the 2.5 km aperture. Data were presented in which the one-hop F2 high ray and low ray exhibited discrete doppler spectra, while two-hop F2 produced a spread doppler spectrum.

B. DISCUSSION AND EVALUATION

It should be mentioned that the ionospheric path used for this study is not necessarily representative of paths elsewhere in the world. First of all, it is located entirely in the midlatitude geographic region, placing it north of ionospheric equatorial effects and south of ionospheric auroral effects. Secondly, the path is oriented nearly perpendicularly to the earth's magnetic field at path midpoint. This tends to minimize the deviative effects of magnetoionic interaction. Finally, the Rocky Mountains provide an unusually rough midpath reflection region.

No specific ionospheric path can really be considered typical. The path studied here is interesting in its features and certainly worthy of study. However, some caution should be exercised before applying these results to other paths.

In addition, the results cited are primarily based upon quiet daytime conditions. Insufficient data are available at present to enable conclusions regarding nighttime or transition periods.

C. CONCLUSIONS

During normal daytime conditions, the performance (azimuthal pattern) of a 2.5 km HF array was not significantly affected by ionospheric reflection of single-hop signals received over a 2600 km path. The performance of the array was substantially degraded, however, when it was receiving multihop modes. This degradation was presumably caused by ground reflections rather than by ionospheric reflections.

Single-hop modes were found to be discrete in time delay, azimuth, and doppler spectra, while multihop modes appeared to be spread in time delay, azimuth and doppler spectra.

D. RECOMMENDATIONS FOR FUTURE WORK

Future work could well be directed toward answering the following questions:

1. How well does a very large array perform for receiving ionospherically propagated signals during nighttime conditions and periods of sunrise and sunset?

2. What is the dependence of the performance of a large array upon path length, magnetic azimuth, and path location?

3. How well does a large array perform in receiving signals propagated via one-hop E layer modes? (The path in the present study was too long for one-hop E propagation.)

4. Will large arrays perform better when receiving multihop modes if the ground reflections occur in other than mountainous regions?

APPENDIX

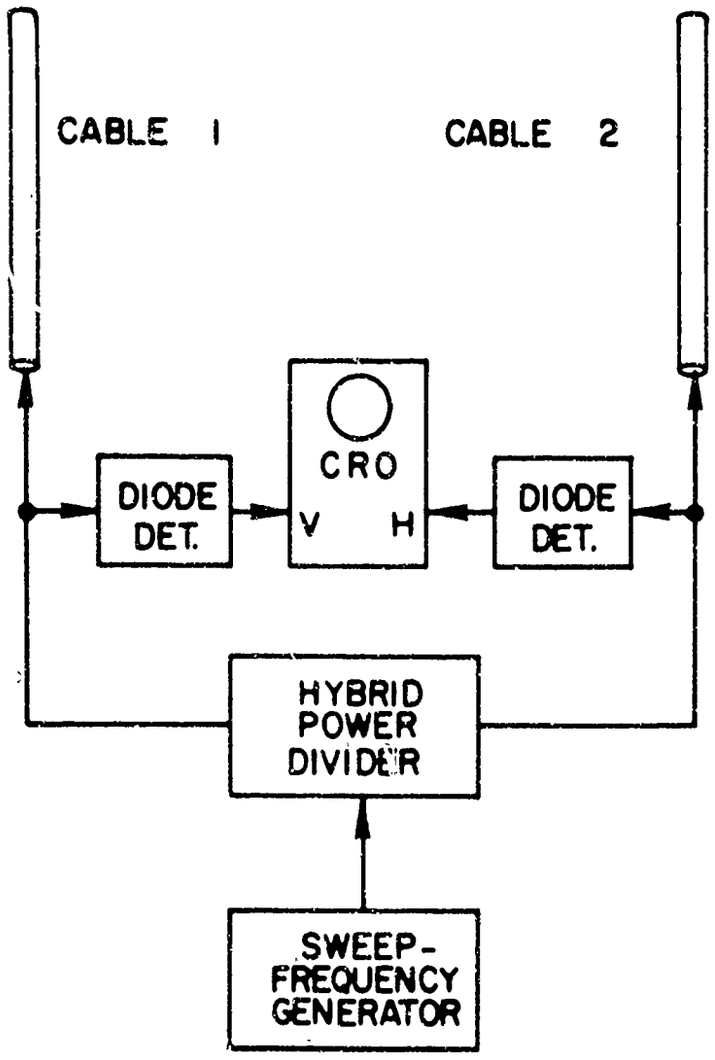

Figure 37 Block diagram of the feedline mat ng system.

Appendix

A NEW TECHNIQUE FOR FEEDLINE MATCHING

One of the most difficult problems in implementing the 2.5 km Los Banos Array consisted of finding a technique which would allow the very long feedlines in the system to be matched in electrical length to sufficient accuracy. This appendix describes a new technique for feedline matching developed by the author to solve this problem.

1. Description of Problem

For a variety of reasons, including a requirement for a low sidelobe level in the array pattern and a desire to measure phase distributions across the array with high accuracy, it was necessary to match the electrical lengths of the array feedlines with very great precision. The exact precision required was established through an error budget to be ± 2.3 deg of phase at 30 MHz or ± 2 in. of length.

As previously described, the Los Banos array is organized into an 8-element array of 32-element subarrays. The element feedlines are 540 ft long and the subarray feedlines are 4300 ft long, so that the signal from each element passes through over 4800 ft of cable before reaching the array output. Hence the requirement for matching feedlines to within ± 2.3 deg of phase at 30 MHz corresponds to matching 4800 ft cables to within 2 in. of the same length.

Since the element ends of the cables are separated by as much as 2.5 km, only the output ends were available for practical measurements, although the element ends could be either open or short-circuited. Thus some form of reflectometry was required. For best accuracy and to insure proper array performance, it was desired to make the cable comparison within the frequency band of interest where round-trip attenuations in the feedlines are over 40 dB. Finally, since there were 264 cables to be cut, the comparison technique had to be both simple and fast.

Of the techniques already available, none seemed satisfactory. This was primarily due to insufficient signal-to-noise ratios resulting from the very large round-trip attenuation. For CW techniques, this meant that the reflected component of the signal was too small to be of use in the presence of the applied signal even when using state-of-the-art directional couplers. In addition, CW techniques are slow and tedious. Pulse techniques require comparison of phases of RF pulses for sufficient accuracy and very high peak powers to get reasonable average powers (signal-to-noise ratios). Providing the necessary peak power and adequately bright displays that could be easily interpreted proved quite difficult.

2. A New Sweep-Frequency Technique of Feedline Matching

The technique developed to solve this problem was a sweep-frequency technique which can be described with the aid of Fig. 37. The output of a linear sweep-frequency generator is split by a hybrid power divider into two identical but isolated signals. These are applied to the inputs of the two cables to be compared. The far ends of the cables are open-circuited. At the input of each line, this arrangement provides both a transmitted signal and a reflected signal the frequencies of which differ by an amount equal to the sweep rate times the round-trip delay of the cable. If the sweep rate and round-trip delay are constant, then the frequency difference will be a constant. When the reflected component is small compared to the transmitted component, the superposition of the two at the cable input will be a wave that fluctuates in amplitude at the difference frequency of the component waves [Ref. 1, p. 569]. This difference frequency may therefore be extracted with a diode detector, and its phase will be a function only of the frequency of the input signal and the length of the cable. Since the input frequencies to each cable are constrained to be the same, any difference in phase of the detected signals can be due only to a difference in cable lengths. These phases are compared using the standard ellipse method of phase measurement [Ref. 28] where the outputs of the two detectors are applied respectively to the vertical and horizontal

plates of an oscilloscope. Then, identical length cables give a straight-line pattern; lines having different lengths give an elliptical pattern whose eccentricity indicates the magnitude of the length difference.

3. Mathematical Description of Technique

To understand this technique more completely, consider the following equations. A linear frequency sweep starting at time zero can be described by

$$f = st + f_o \tag{A.1}$$

where

- f is the frequency (Hz)
- s is the sweep rate or the rate of change of frequency with time (Hz/sec)
- t is time (sec)
- f_o is the sweep starting frequency (Hz) (frequency when $t = 0$).

Hence, a sweep frequency CW (SFCW) signal, $v(t)$, can be described by

$$v(t) = \cos \varphi(t)$$

where its phase, $\varphi(t)$, is given by 2π times the integral with respect to time of Eq. (A.1), or

$$\varphi(t) = 2\pi \left(\tfrac{1}{2} st^2 + f_o t\right) + \varphi_o \quad , \tag{A.2}$$

where φ_o is the phase at $t = 0$.

If $v(t)$ is transmitted into an open circuited cable having a one-way time delay τ and an attenuation factor α, both the transmitted signal and a reflected signal $v(t + 2\tau)$ will be present at the cable input, and the superposition, $u(t)$, will be

$$u(t) = v(t) + v(t + 2\tau) = \cos \varphi(t) + \alpha^2 \cos \varphi(t + 2\tau) \quad .$$

From trigonometry, this can be written as

$$u(t) = A \cos [\varphi(t) + \psi] \quad ,$$

where

$$A = \sqrt{1 + \alpha^4 + 2\alpha^2 \cos \Delta\varphi} \tag{A.3}$$

$$\psi = \tan^{-1} \frac{\alpha^2 \sin \Delta\varphi}{1 + \alpha^2 \cos \Delta\varphi}$$

$$\begin{aligned} \Delta\varphi &= \varphi(t + 2\tau) - \varphi(t) \\ &= 4\pi [st + s\tau + f_o] \tau \quad . \end{aligned} \tag{A.4}$$

Consequently, the signal at the cable input can be expressed as a sweep-frequency signal with a low frequency envelope, A, and a low-frequency phase modulation, ψ. A diode detector can then extract the envelope, A, which has a fundamental frequency of $2\ s\tau$ and a constant phase component of $s\tau^2 + f_o\tau$. Using Eq. (A.4) and the subscripts 1 and 2 to distinguish parameters associated respectively with cables 1 and 2 of Fig. 37, the phase difference between the two detected envelopes will be

$$\Delta\varphi_2 - \Delta\varphi_1 = 4\pi [st + s(\tau_1 + \tau_2) + f_o] (\tau_2 - \tau_1) \quad . \tag{A.5}$$

Since $s\tau_1$ and $s\tau_2$ are usually quite small compared to f_o, this equation can be simplified to

$$\Delta\varphi_2 - \Delta\varphi_1 \approx 4\pi\,(st + f_o)\,(\tau_2 - \tau_1) \quad . \tag{A.6}$$

Notice that when the time-delay difference is finite the phase difference displayed on the oscilloscope varies with time. Typically the bandwidth swept is less than 10 percent of f_o, however, so that the change in the pattern is small, and the difference in cable lengths can easily be estimated from the ellipse eccentricity and Eq. (A.6). When the cables are the same length the pattern displayed will be a straight line regardless of the bandwidth swept.

Notice that no restrictions were placed on the cable attenuation in deriving Eq. (A.6). When the attenuation is large $(\alpha < 0.3)$, the case where this technique surpasses most others, Eq. (A.3) becomes

$$A \approx 1 + \alpha^2 \cos \Delta\varphi \quad .$$

In each detector the undesired dc component can be removed by appropriate filtering or a dc bias, leaving only the desired ac component $(\alpha^2 \cos \Delta\varphi)$ applied to the oscilloscope. The display will be a straight line for equal length cables, and an ellipse whose eccentricity indicates the length difference for unequal cables.

Although a linear-frequency sweep was assumed for simplicity in the above discussion, virtually any form of frequency sweep will provide a straight-line pattern for identical length lines and an open pattern for unequal lines. The linear sweep has the advantage that it produces constant envelope frequencies which are easier to separate from the dc component. In addition, the oscilloscope patterns have a uniform intensity over the entire sweep, making them easy to interpret. But it should be emphasized that the requirement for linearity is not at all

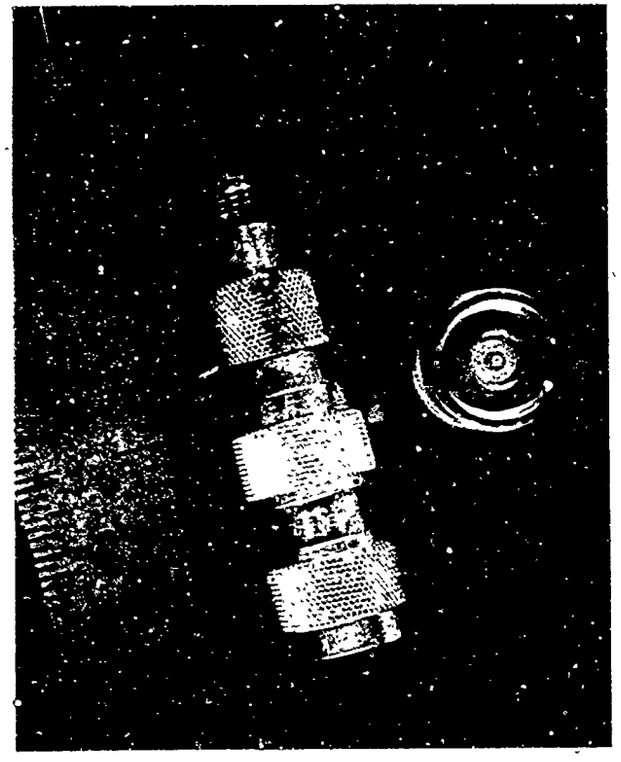

ADAPTER USED TO LENGTHEN CABLE

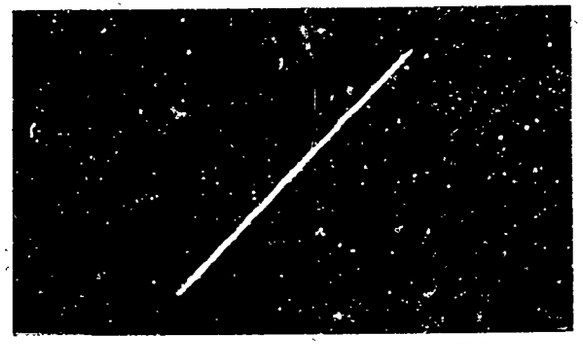

DISPLAY FOR CABLES OF EQUAL LENGTH

DISPLAY FOR ADAPTER IN SERIES WITH ONE CABLE

Figure 38 Demonstration of the sensitivity of the feedline matching technique when comparing two 4800 ft feedlines.

Upper Right: Display for equal length cables.
Lower Right: Display when the adapter shown at the left was connected in series with one of the cables.

severe. When the attenuation is low $(1 \geq \alpha \geq 0.3)$ the envelope, A, has strong harmonics (when $\alpha = 1$, A is a full-wave rectified sine wave), and the oscilloscope display will in general be a distorted ellipse. However, equal length lines will still produce a straight-line pattern, and the difference in length of unequal lines will still be indicated by the shape of the pattern.

4. Example of Technique Performance

When matching the feedlines in the Los Banos Array the SFCW signal used was a sawtooth in frequency sweeping from 24 MHz to 26 MHz at a rate of 1 MHz/sec every 2 sec. The sensitivity of the technique when matching two 4800 ft feedlines is illustrated by Fig. 38. The straight-line display for two equal length cables is shown at the upper right of this figure. Exchanging cables produced no change in this display, an excellent check on the system accuracy. When the adapter shown at the left was connected in series with one of the cables, the display became the ellipse shown at the lower right. The eccentricity of this ellipse indicates that the cables differed in length by 2.9 in. of free space, in exact agreement with independent CW measurements of the electrical length of the adapter. In this case the cables had 40 dB of round-trip attenuation for these frequencies.

Using this technique, there was no difficulty in matching the lengths of the feedlines in the Los Banos array to the required tolerance. In addition, the technique was found to be extremely fast and convenient in practice.

REFERENCES

1. F. E. Terman, Electronic and Radio Engineering, Fourth Ed., McGraw-Hill Book Co., Inc., New York, 1955.

2. E. C. Hayden, "Propagation Studies Using Direction-Finding Techniques," J. Res. NBS, 65D, 3, May-Jun 1961, pp. 197-212.

3. P. J. D. Gething, "High-Frequency Direction Finding," Proc. IEE, 113, 1, Jan 1966, pp. 49-61.

4. S. A. Bowhill, "Diversity Effects in Long Distance High Frequency Radio Pulse Propagation," J. Res. NBS, 65D, 3, May-Jun 1961, pp. 213-223.

5. J. Ames, "Spatial Properties of the Amplitude Fading of Continuous HF Radio Waves," Radio Science, 68D, 12, Dec 1964, pp. 1309-1318.

6. E. N. Bramley and W. Ross, "Measurements of the Direction of Arrival of Short Radio Waves Reflected at the Ionosphere," Proc. Roy. Soc., A, 207, Jun 1951, pp. 251-267.

7. E. N. Bramley, "Direction-Finding Studies of Large-Scale Ionospheric Irregularities," Proc. Roy. Soc., A, 220, Oct 1953, pp. 39-61.

8. E. N. Bramley, "Some Comparative Directional Measurements on Short Radio Waves Over Different Transmission Paths," Proc. IEE, 102B, 4, Jul 1955, pp. 544-549.

9. E. N. Bramley, "Directional Observations on H.F. Transmissions Over 2100 km," Proc. IEE, 103B, 9, May 1956, pp. 295-300.

10. W. C. Bain, "Phase Difference Observations at Spaced Aerials and Their Application to Direction Finding," J. Res. NBS, 65D, 3, May-Jun 1961, pp. 229-232.

11. H. Jasik, Ed., Antenna Engineering Handbook, McGraw-Hill Book Co., Inc., New York, 1961, Chap. 2, pp. 36-41.

12. L. H. Tveten and R. D. Hansucker, "Remote Sensing of the Terrestrial Environment with an HF Radio High-Resolution Azimuth and Elevation Scan System," Proc. IEEE, 57, 4, Apr 1969, pp. 487-493.

13. F. A. Polkinghorn, "A Single Sideband Musa Receiving System for Commercial Operation on Transatlantic Radio Telephone Circuits," Proc. IRE, 28, Apr 1940, pp. 157-170.

Preceding page blank

REFERENCES (Cont)

14. H. Brueckmann and R. Silberstein, "HF Propagation Test of ISCAN," IEEE Trans. Antennas and Propagation, AP-11, Jul 1963, pp. 454-458.

15. M. Balser and W. B. Smith, "Some Statistical Properties of Pulsed Oblique HF Ionospheric Transmissions," J. Res. NBS, 66D, 6, Nov-Dec 1962, pp. 721-730.

16. L. E. Sweeney, Jr., "Experimental Measurements of Amplitude and Phase Distributions Across a 2.5 km HF Array," presented at the Spring URSI Meeting, Washington, D. C., 1968.

17. J. M. Lomasney, L. E. Sweeney and R. B. Fenwick, "Studies of Ionospheric Propagation Related to High-Frequency Radio Broadcasting," Report SEL-69-009 (TR No. IA-7), Stanford Electronics Laboratories, Stanford, Calif., Feb 1969.

18. J. D. Kraus, Antennas, McGraw-Hill Book Co., Inc., New York, 1950, pp. 97-110.

19. L. E. Sweeney, Jr., "Comparison of Electrically-Long Lines Using Swept-Frequency Reflectometry," presented at the Fall URSI Meeting, Boston, Mass., 1968.

20. L. L. Peden, J. M. Lomasney and R. B. Fenwick, "A Flexible, HF Sweep-Frequency Sounder With Submicrosecond Resolution," Report SEL-68-088 (TR No. 140), Stanford Electronics Laboratories, Stanford, Calif., Nov 1968.

21. J. W. Wright and L. A. Fine, "Mean Electron Density Variations of the Quiet Ionosphere 2 - April 1959," NBS Technical Note No. 40-2, Boulder Laboratories, U. S. Dept. of Commerce, Washington D. C., Feb 1960, p. 24.

22. R. M. Jones, "A Three-Dimensional Ray-Tracing Computer Program," Radio Science, 3, 1, Jan 1968, pp. 93-94.

23. T. A. Croft, "Interpreting the Structure of Oblique Ionograms," Report SEL-66-010 (TR No. 114), Stanford Electronics Laboratories, Stanford, Calif., Feb 1966.

24. A. C. Phillips, "A Single-Antenna Repeater for HF Radio Propagation Studies," Report SEL-69-064 (TR No. 154), Stanford Electronics Laboratories, Stanford, Calif., Oct 1969.

25. W. T. Cochran, et. al., "What is the Fast Fourier Transform?," IEEE Trans. Audio and Electroacoustics, AU-15, 2, Jun 1967, pp. 45-55.

REFERENCES (Cont)

26. R. N. Bracewell, The Fourier Transform and Its Applications, McGraw-Hill Book Co., Inc., New York, 1965.

27. R. B. Blackman and J. W. Tukey, The Measurement of Power Spectra, Dover Publications, Inc., New York, 1958.

28. F. E. Terman and J. M. Pettit, Electronic Measurements, McGraw-Hill Book Co., Inc., 1952, p. 267.

UNCLASSIFIED
Security Classification

DOCUMENT CONTROL DATA - R & D

(Security classification of title, body of abstract and indexing annotation must be entered when the overall report is classified)

1. ORIGINATING ACTIVITY (Corporate author)
Stanford Electronics Laboratories, Stanford, Univ.
Stanford, Calif.

2a. REPORT SECURITY CLASSIFICATION
Unclassified

2b. GROUP

3. REPORT TITLE
SPATIAL PROPERTIES OF IONOSPHERIC RADIO PROPAGATION AS DETERMINED WITH HALF-DEGREE AZIMUTHAL RESOLUTION

4. DESCRIPTIVE NOTES (Type of report and inclusive dates)
Technical Report

5. AUTHOR(S) (First name, middle initial, last name)
Sweeney, L. E. Jr.

6. REPORT DATE
June 1970

7a. TOTAL NO. OF PAGES
91

7b. NO. OF REFS
28

8a. CONTRACT OR GRANT NO.
ONR Nonr-225(64)

b. PROJECT NO.
NR 088-019 &

c.
ARPA Order No. 196

d.

9a. ORIGINATOR'S REPORT NUMBER(S)
Technical Report No. 155
SU-SEL-70-034

9b. OTHER REPORT NO(S) (Any other numbers that may be assigned this report)

10. DISTRIBUTION STATEMENT
Approved for public release and sale; its distribution is unlimited

11. SUPPLEMENTARY NOTES

12. SPONSORING MILITARY ACTIVITY
Office of Naval Research

13. ABSTRACT
In order to determine the influence of oblique ionospheric radio propagation upon the performance (azimuthal pattern) realized by a very large HF array, a 256-element, 2.5 km broadside array has been constructed, and used to receive signals propagated over a 2600 km east-west path from a test transmitter. During implementation of this array, a new technique for matching the lengths of very long feedlines was devised and shown to provide outstanding precision and convenience. It was found that the sensitivity conferred by sweep-frequency CW (SFCW) sounding and the directivity of the receiving array permitted useful ionospheric research to be conducted with transmitted powers as low as 5 mW. Through the use of SFCW sounding, propagation modes were separated and their azimuthal properties were individually studied as a function of radio frequency with the large array. Daytime studies revealed that single-hop propagation usually appears discrete in azimuth and time delay within the resolution of the system. Ground-reflected modes, on the other hand, are generally spread both in azimuth and time delay, presumably as a consequence of the ground reflections occurring within the Rocky Mountain region. During quiet conditions, the one-hop F2 high ray was found to commonly arrive south of the low ray. This tendency was hypothesized to be a consequence of ionospheric tilts having north-south slopes which increase with altitude. The plausibility of this explanation was confirmed by three-dimensional computer raytracing with a model ionosphere based upon vertical ionosonde data. A new propagation mode was discovered which is thought to result from two-hop propagation in which energy travels one hop via high ray and the other via low ray. The existence of such a "combination mode" requires rough scattering at the midpath reflection region (the Rocky Mountins in this case), to enable transfer of energy between high and low
(see other side)

DD FORM 1 NOV 65 1473

UNCLASSIFIED
Security Classification

14 KEY WORDS	LINK A ROLE	LINK A WT	LINK B ROLE	LINK B WT	LINK C ROLE	LINK C WT
HIGH-FREQUENCY						
OBLIQUE IONOSPHERIC PROPAGATION						
SWEEP-FREQUENCY SOUNDING						
WIDE-APERTURE						
BROADSIDE ARRAY						
DIGITAL BEAMFORMING						
AZIMUTHAL MODE DISTRIBUTION						

Abstract (Contd)

rays. The proposed explanation for the combination mode was substantiated analytically by computer ray-tracing, and experimentally by operating an HF repeater at the path midpoint. A new experimental technique was developed which, using SFCW sounding, measures amplitude versus time delay at eight azimuths simultaneously, with each azimuth having the resolution of the full 2.5 km array. The new technique makes extensive use of digital processing, and allows greatly improved flexibility, accuracy and dynamic range compared to previous techniques. In addition, the technique allows the distributions across the array of received signal amplitude and phase to be measured individually for all propagation modes. Finally, measurement of ionospherically induced doppler shifts versus azimuth for obliquely propagating CW signals demonstrated that, when modes could be resolved in frequency on the basis of their different doppler shifts, they could often be identified on the basis of their azimuthal properties. This was accomplished when receiving with only eight whips spaced uniformly across the 2.5 km aperture. Data were presented in which the one-hop F2 high ray and low ray exhibited discrete doppler spectra, while two-hop F2 produced a spread doppler spectrum.

It was concluded that, during normal daytime conditions, the performance (azimuthal pattern) of a 2.5 km HF array was not significantly affected by ionospheric reflection of single-hop signals received over a 2600 km path. The performance of the array was substantially degraded, however, when it was receiving multihop modes. This degradation was presumably caused by ground reflections rather than by ionospheric reflections.